UNC13B – A potential target gene of 9p13.3 amplicon in prostate cancer

Master´s thesis

Anni Vesamäki

University of Tampere

BioMediTech

May 2015

ACKNOWLEDGEMENTS

The practical and written parts of this thesis were done in the Molecular Biology of Prostate Cancer Group, BioMediTech (BMT), University of Tampere. First, I would like to thank Professor Tapio Visakorpi for giving me the opportunity to work in his research group during several summers and during the practical work of this thesis. I would like to also thank all the members of the research group for their great advices and memorable times together.

Especially, I would like thank my lovely supervisor PhD Leena Latonen for her quidance, experience and patience during this process. I also want to thank technicians Mariitta Vakkuri and Päivi Martikainen for their technical and practical help in the laboratory. Especially Mariitta, who´s memory will always stay in my heart.

I would like to thank my family for all the support during these many years of studies. Especially my beloved husband who persistently pushed me forward and never stopped believing me, and my two gorgeous daughters who are the light of my life.

Tampere, May 2015
Anni Vesamäki

PRO GRADU-TUTKIELMA
Paikka: Tampereen yliopisto
BioMediTech
Tekijä: VESAMÄKI, ANNI MARIA
Otsikko: *UNC13B* – A potential target gene of 9p13.3 amplicon in prostate cancer
Sivut: 57 sivua, 1 liitesivu
Ohjaajat: Professori Tapio Visakorpi ja FT Leena Latonen
Tarkastajat: Professorit Markku Kulomaa ja Tapio Visakorpi
Aika: Toukokuu 2015

TIIVISTELMÄ

Tutkimuksen tausta ja tavoitteet: Eturauhassyöpä on miesten yleisin syöpä länsimaissa. Se on erittäin heterogeeninen sairaus niin kliinisesti kuin geneettisestikin. Eturauhassyöpään liittyy lukuisia genomin uudelleen järjestäytymisiä, joista yleisimpiä ovat kromosomialueiden kopiolukumuutokset. Eräs hiljattain löydetty toistuva monistunut kromosomialue on 9p13.3. Tämän tutkimuksen tavoitteena oli tutkia voisiko *UNC13B* olla tämän uuden kromosomi-monistuman kohdegeeni eturauhassyövässä. Tämä työ on osa laajempaa 9p-kromosomi-alueen tutkimusta.

Tutkimusmenetelmät: *UNC13B*:n ilmentyminen määritettiin lähetti-RNA-tasolla (mRNA) kvantitatiivisella käänteiskopiointipolymeraasiketjureaktiolla (RT-qPCR) eri eturauhassyöpä-solulinjoista. PC-3-, MCF-7- ja LNCaP-solulinjat transfektoitiin väliaikaisesti *UNC13B*-cDNA:lla, ja yli-ilmentyminen varmistettiin mRNA-tasolla RT-qPCR:lla sekä proteiinitasolla immunoblottauksen ja –sytokemian avulla. UNC13B:n toimintaa tutkittiin yli-ilmentämällä sitä PC-3- ja MCF-7-soluissa, ja analysoimalla yli-ilmentymisen vaikutusta solujen jakautumis- ja migraatiokykyyn. Näiden tutkimusten lisäksi UNC13B:n ilmentyminen määritettiin kliinisistä eturauhassyöpänäytteistä RT-qPCR:n ja immunohistokemian avulla.

Tutkimustulokset: *UNC13B*-geenin ilmentymistasot vaihtelivat eri syöpäsolulinjojen välillä. *UNC13B*:n yli-ilmentyminen PC-3-soluissa lisäsi jonkin verran solujen jakautumista, mutta toisaalta yli-ilmentymistaso osoittautui matalaksi tässä solulinjassa. Yli-ilmentymisellä ei ollut vaikutusta PC-3-solujen migraatiokykyyn. *UNC13B*:n yli-ilmentymisen vaikutusta MCF-7-solujen jakautumiseen oli haastavaa tutkia, sillä solut tuottivat epätavallisen suuren määrän UNC13B-proteiinia transfektiolla aiheuttaen solukuolemaa. Tulokset kliinisten eturauhassyöpänäytteiden analyysistä viittaavat, että korkeammalla *UNC13B*-geenin ilmentymisellä saattaa olla rooli edistyneemmässä eturauhassyövässä vaikkakaan tulokset eivät ole tilastollisesti merkittäviä. Hormonirefraktorisissa (HR) näytteissä esiintyi korkein *UNC13B*:n ilmentymisen keskiarvo verrattuna näytteisiin eturauhasen hyvänlaatuisesta liikakasvusta ja primaarisyövästä. Muutamassa HR-näytteessä havaittiin myös erityisen korkea *UNC13B*-ilmentyminen mRNA-tasolla.

Johtopäätökset: Kliinisten eturauhassyöpänäytteiden analyysin tulokset viittaavat siihen, että korkeammat *UNC13B*-ilmentymistasot saattavat liittyä edistyneempiin syöpätapauksiin ja/tai syövän etenemiseen. UNC13B-geenin ilmentymisprofiilin voisi täten yhdistää muihin parametreihin eturauhassyövän aggressiivisuuden ennustamisessa. UNC13B:n toiminnallinen rooli syöpäsoluissa ei selvinnyt tässä tutkimuksessa. Lisää tutkimuksia tarvitaan selvittämään UNC13B:n potentiaalista roolia eturauhassyövän ennustettavuuden biomarkkerina.

MASTER´S THESIS
Place: University of Tampere
BioMediTech
Author: VESAMÄKI, ANNI MARIA
Title: *UNC13B* – A potential target gene of 9p13.3 amplicon in prostate cancer
Pages: 57 pages, 1 appendix page
Supervisors: Professor Tapio Visakorpi and Dr. Leena Latonen
Reviewers: Professors Markku Kulomaa and Tapio Visakorpi
Date: May 2015

ABSTRACT

Backround and aims: Prostate cancer is the most common cancer in men in Western countries. It is a highly heterogeneous disease both clinically and genetically. Multiple genomic rearrangements are associated with the disease, copy number alterations being the most common ones. One recently found recurrently amplified chromosomal region is 9p13.3. The aim of this thesis was to study whether *UNC13B* is a potential target gene of this novel amplification in prostate cancer. This thesis is part of a broader study of 9p chromosomal region in prostate cancer.

Methods: The expression of endogenous *UNC13B* mRNA was determined with RT-qPCR from different prostate cancer cell lines. PC-3, MCF-7 and LNCaP cancer cells were transiently transfected with *UNC13B.* Overexpression was verified by RT-qPCR analysis at mRNA level, and by immunoblotting and immunocytochemistry at protein level. The functional role of UNC13B was studied by overexpressing *UNC13B* in PC-3 and MCF-7 cells, and assaying the effect on cell growth and migration ability. In addition, the expression of UNC13B was determined from clinical prostate cancer specimens by using RT-qPCR and immunohistochemistry.

Results: The levels of *UNC13B* overexpression showed variability in studied cell lines. Overexpression of *UNC13B* slightly increased the proliferation of PC-3 cells; however the overexpression status proved to be low in PC-3 cells. Overexpression did not affect migration ability of PC-3 cells. The effect of *UNC13B* overexpression on MCF-7 cell growth was a challenge to determine since the cells exhibited abnormally large amounts of UNC13B protein upon transfection causing cell death. The results from clinical tumor sample analyses suggest that higher *UNC13B* expression might have a role in more advanced disease although the results were not statistically significant. Compared to benign prostatic hyperplasia and primary prostate cancer, the hormone refractory cancer samples showed the highest mean expression and also a few cases of particularly high *UNC13B* expression at mRNA level.

Conclusion: The results from clinical samples analyses indicate that higher *UNC13B* expression levels might be associated with more advanced disease and/or disease progression. This suggests that *UNC13B* expression profile could potentially be combined with other parameters to predict the aggressiveness of the disease. The functional role of UNC13B in cancer cells remains a question. More studies are needed to assess the potential use of *UNC13B* as a prognostic biomarker.

CONTENTS

ABBREVIATIONS

aCGH	Array CGH
AKT	V-akt murine thymoma viral oncogene homolog
AR	Androgen receptor
ATCC	American Type Culture Collection
BPH	Benign prostatic hyperplasia
C9orf25	Chromosome 9 open reading frame 25
CDC34	Cell division cycle 34
cCGH	Chromosomal CGH
CGH	Comparative genomic hybridization
CRPC	Castration resistant prostate cancer
DAG	Diacylglycerol
DAPI	4',6-diamidino-2-phenylindole
DBSs	DNA double-strand breaks
DCTN3	Dynactin 3
DTT	Dithiothreitol
E2R2	Ubiquitin-conjugating enzyme
ERG	ETS-related gene, v-ets erythroblastosis virus E26 oncogene homolog
ETS	Erythroblast transformation specific
FISH	Fluorescence in situ hybridization
FOXA1	Forkhead box A1 transcription factor
GALT	Galactose-1-phosphate uridylyltransferase
HGPIN	High-grade PIN
HER2	Human epidermal growth factor receptor 2
HRP	Horseradish peroxidase
HRPC	Hormone-refractory (hormone-resistant) prostate cancer
IHC	Immunohistochemistry
IL-11RA	Interleukin 11 receptor alpha subunit
MLL2	H3K4-specific histone methyltransferase
MYC	v-myc myelocytomatosis viral oncogene homolog
NCOA2	Nuclear receptor coactivator 2
NP-40	Nonyl phenoxypolyethoxylethanol
PIGO	Phosphatidylinositol glycan anchor biosynthesis, class O
PIN	Prostatic intraepithelial neoplasia
PMSF	Phenylmethylsulfonyl fluoride
PTEN	Phosphatase and tensin homolog
RB1	Retinoblastoma 1 tumor suppressor gene
RT-qPCR	Real-time reverse transcription quantitative PCR
SPOP	Speckle-type POZ protein
TBP	TATA-binding protein
TBS	Tris-buffered saline
TMPRSS2	Transmembrane protease, serine 2
TOP2B	Topoisomerase 2B
TP53	Tumor protein 53
UBAP	Ubiquitin-associated protein
UBE2R2	Ubiquitin-conjugating enzyme E2R 2
UNC13B	Unc-13 homolog B

VCP	Valosin containing protein
WDR40A	WD repeat-containing protein 40A
PFA	Paraformaldehyde
PIN	Prostatic intraepithelial neoplasia
PMSF	Phenylmethylsulfonyl fluoride
PSA	prostate specific antigen
PTEN	Lipid-protein phosphatase

1. INTRODUCTION

Prostate cancer is the most common cancer in men, both in Finland and other Western countries. In 2007 – 2011 in Finland, nearly 4500 new cases were diagnosed annually and 824 cancer related deaths were registered annually (www.cancer.fi/syoparekisteri/en/; 16.12.2013). Like in other cancers, the incidence of prostate cancer is growing. This is largely caused by ageing of the population and improved screening and diagnostic methods. Increasing number of men is being diagnosed with very early stage prostate cancer due to the widespread use of prostate specific antigen (PSA) testing.

The risk of prostate cancer is strongly age related. Approximately 40% of men over age of 50 have slow-growing and well-differentiated prostate cancer; of these cancers, approximately 10% become clinically significant and only 3% contribute to cause of death (Haas et al., 2008). In general, most of the cases are diagnosed in the age range of 70 to 74. The survival ratio of prostate cancer is rather good because most men diagnosed at a very early stage will die with prostate cancer but not from it (Hughes C et al., 2005). The 5-year survival ratio in Finland registered in 2007 - 2011 was 97% (www.cancer.fi/syoparekisteri/en/; 16.12.2013).

Prostate cancer is a highly heterogeneous disease in both clinically and genetically. Typical feature for prostate cancer is slowly growing tumors which cause no life-threatening condition for patients. Also the disease metastasizes rarely. However, some prostate tumors are highly aggressive, metastasize early and ultimately develop to castration resistant prostate cancer (CRPC) with only limited treatment options. One of the key questions in the prostate cancer research and in clinics nowadays is how to distinguish aggressive tumor types from the indolent ones at early stage. This could be achieved by identifying potential biomarker genes which are involved in prostate cancer progression.

Prostate cancer is associated with multiple genetic alterations, including somatic point mutations and variable genomic rearrangements. Genetic heterogeneity of the disease can be seen between patients and within a patient; prostate cancer is often multifocal meaning as many as 5 to 6 tumors with different genetic profiles occurring in a single prostate. In general, somatic point mutations are relatively rare compared to other cancers while gene copy number

alterations are much more common (Taylor et al., 2010). Furthermore, gene fusions are relatively common, most frequent being TMRPSS2:ERG fusion (Pettersson et al., 2012).

A novel recurrent amplification in the chromosomal region 9p13.3 has been detected in prostate cancer (Saramaki et al., 2006; Taylor et al., 2010). According to previous studies, 10% and 33% of prostatectomy treated patients gain high-level and low-level amplifications, respectively (Leinonen, 2007). Of hormone-refractory tumors, 14% contain high-level amplification and and 44% low-level amplification (Leinonen, 2007). The novel amplicon contains multiple target genes whose expression correlates with increased copy number, however, no cancer associated genes have been identified so far (Leinonen, 2007). In this research, one of these potential candidate genes, *UNC13B*, was studied in more detail in order to see whether it could be the target gene of 9p13.3 amplicon and whether it could be used as a new prognostic marker for prostate cancer.

2. REVIEW OF LITERATURE

2.1 Prostate cancer

Prostate cancer arises from prostate gland located in the male pelvis between the bladder and the penis (Figure 1). The walnut-sized prostate gland belongs to the accessory sex gland system in males that synthesizes and secretes many components of the seminal plasma including male sex hormones. It is believed that the spermatozoa survival in the female reproductive tract is largely enhanced by prostatic secretions although fertilization isn´t dependent on prostatic fluids.

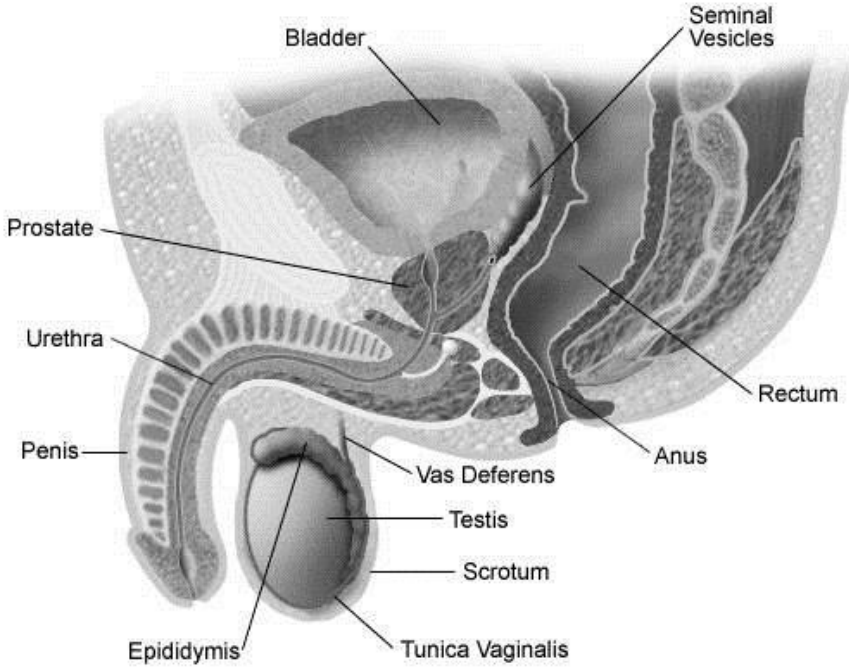

Figure 1. The prostate gland. The prostate gland is located below the bladder, just in front of the rectum, and it surrounds the urethra. Picture is modified from http://prostate-health-net.com/prostate_picture.html (20.02.2015).

2.1.1 Anatomy of the prostate

Prostate gland can be divided into four zones: peripheral zone, central zone, anterior fibro-muscular zone, and preprostatic region (Young & Heath, 2000) (Figure 2). The zonal anatomy of the prostate was developed and reported by McNeal in 1981 (McNeal JE, 1981), and it allows the assignment of the zone of origin to individual prostate cancer foci. A fibroelastic

band, rather than a capsule, encloses the posterior and lateral surfaces of the prostate gland while fibro-muscular stroma surrounds the apical and anterior parts (Raychaudhuri B et al., 2008). The anterior fibro-muscular stroma lacks entirely glandular elements. Instead, it consists of connective tissue and both smooth and skeletal muscle. Peripheral zone constitutes over 70% of the glandular prostate and almost all (68%) carcinomas arise here (McNeal JE, 1981). The peripheral zone consists of pseudostratified secretory epithelium with columnar cells and basal cells which are supported by a fibroelastic stroma. When peripheral zone surrounds the distal urethra, the central zone (25% of the glandular prostate) surrounds the ejaculatory ducts.

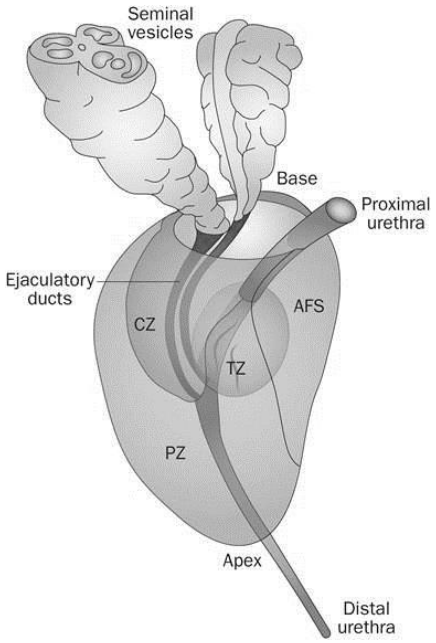

Figure 2. View of the prostate gland and urethra. Prostate gland is divided into three zones: the central zone (CZ), the transition zone (TZ) and the peripheral zone (PZ). The seminal vesicles and ejaculatory ducts are located at the base of the prostate. The anterior fibromuscular stroma (AFS) is located anteriorly. Picture is modified from Wein AJ, Campbell-Walsh Urology 9th Edition, 2007.

The central zone is a region rarely associated with carcinoma. However, there are suggestions that small percentage of tumors arising from this region tend to be more aggressive than peripheral zone cancers with a far greater risk of extracapsular extension and seminal vesicle invasion (Cohen RJ et al., 2008). The preprostatic region including the periurethal ducts and transition zone is the smallest of the four zones. The small ducts in the transition zone are the exclusive site of benign prostatic hyperplasia (BPH) and about 24% of prostate cancers arise from this region (McNeal JE, 1981).

Over 95% of prostate cancers are adenocarcinomas that arise from prostatic epithelial cells (Verhagen PC et al., 2002). Like in all carcinomas, the differentiated epithelial cells transform through activation of oncogenes and loss of tumor suppressor genes, which leads to a growth and survival advantage (Taichman RS et al., 2007). However, prostate carcinogenesis is not only a result of DNA damage that occur in epithelial cells, it is a result of complex interplay of genes, the cellular microenvironment, the macroenvironment of the host, and the environment where the host resides (Toivanen et al., 2012). Multiple genetic changes have been associated with prostate cancer, however the genetic changes which will eventually lead to tumorigenesis are not well understood.

2.1.2 Tumorigenesis

At first, prostatic intraepithelial neoplasia (PIN) lesions will form that are characterized by the proliferation of secretory cells and loss of distinct basal and secretory layers (Schulz WA et al., 2003). PINs are graded as low-grade (LGPIN) to high-grade (HGPIN) according to the severity of dysplasia of the epithelial cells, and especially HGPIN resembles prostate cancer (Montironi R et al., 2011). According to many studies of animal models and man, PIN is the only accepted precursor of prostatic adenocarcinoma (Bostwick DG et al., 2012; Montironi R et al., 2011). Similarities between PIN and cancer are nuclear and nucleolar enlargement, partial basal cell layer distruption indicating possible stromal invasion, multifocality and similar zonal distribution (Bostwick DG et al., 2012). In addition, PIN and prostate cancer have comparable genetic alterations (Bostwick DG et al., 2012) with a difference that cancer obtains more of these changes.

2.1.3 Gleason grading system

Prostate adenocarcinomas are typically graded by patterns of gland formation in order to determine the degree of differentiation. Grading systems are used in cancer diagnostics and prognostics to evaluate the differentiation and aggressiveness of the cancer. A widely accepted method for grading the histological differentiation of prostate cancer is Gleason grading system developed by Donald F Gleason in the late 60´s (Figure 3). This system is based on two levels of scoring because of the histological variation within each tumor (Harnden P et al., 2007). The most prominent histologic pattern and the second most common pattern are both assigned a grade of 1 to 5. These two grades are then summed and reported as the total Gleason score. A low Gleason score (<6) is considered as a more indolent

malignancy with a good prognosis whereas a high Gleason score (>8) is associated with an aggressive biological behavior and a potential risk of systemic disease. Gleason grading system is less successful in the prognosis of moderately differentiated cancers (Gleason score 5-7).

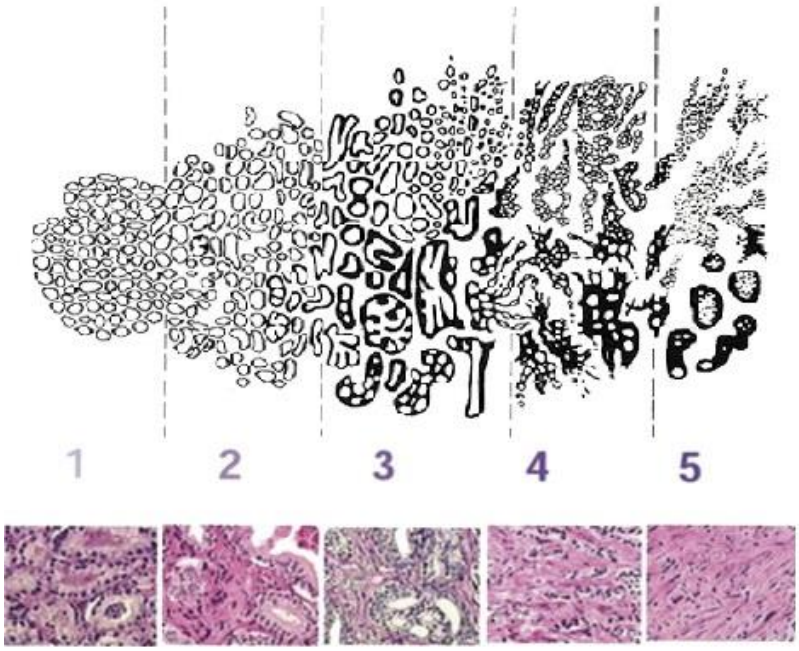

Figure 3. Schematic diagram of Gleason grading system. Numbers refer to Gleason grades. Above are the original Dr. Gleason´s drawing of each grade and below are the corresponding HE stained micrographs for each grade. Picture is modified from Harnden et al., 2007.

2.1.4 Non-malignant prostate diseases

There are different types of non-cancerous problems of the prostate including prostatitis and benign prostatic hyperplasia (BPH). Prostatitis is the most common prostate problem in men under the age of 50 and it is defined as inflammation of the prostate gland. In Finland, the overall lifetime prevalence of prostatitis is 14.2% (Mehik et al., 2000) while the overall prevalence rate is 5-9% (Jiang et al., 2013). Prostate inflammation can be caused by bacterial infection, such as common *Escherichia coli*, and the infection can be either acute or chronic. Prostatitis can also occur as inflammatory chronic pelvic pain syndrome in the absence of known infecting organism, or noninflammatory syndrome where both inflammation and infection-fighting cells are missing. Asymptomatic inflammatory prostatitis lacks common symptoms of prostatitis, such as urination difficulties, fever, lower back and/or pelvic pain, but inflammatory cells are still present. There are suggestions that the high prevalence of prostatitis could contribute to prostate carcinogenesis since the free radicals produced by

inflammation tissue increases the cancer risk by suppressing antitumor activity (Lonkar & Dedon, 2011).

Benign prostatic hyperplasia (BPH) is also a common urological condition in men older than 60 caused by the non-cancerous enlargement of the prostate (Russo et al., 2014). The oversized prostate can block urethra and cause multiple lower urinary tract symptoms such as difficulty in the beginning of urination and the need to frequently empty the bladder, especially during night time. BPH can be treated by active surveillance if the symptoms are mild or by medical therapies such as alpha blockers or 5α-reductase inhibitors if the patient is bothered by the symptoms (Wang et al., 2014). The aim of the drug treatment is to improve the quality of life of the patient by relieving the symptoms and slowing down the clinical progression of the disease (Wang et al., 2014).

Although according to present knowledge, BPH is a non-malignant condition and not a precursor of prostate cancer, there seems to be some association between these two conditions. They are both among the most common diseases of the prostate gland and share some features such as hormone-dependent growth and response to antiandrogen therapy (Orsted & Bojesen, 2013). Also chronic inflammation and metabolic disruption are common risk factors for both diseases (Orsted & Bojesen, 2013). The important differences between BPH and prostate cancer include histological and localization aspects. BPH is most often localized in the transition zone of the prostate gland and histologically defined as the hyperplasia of the stromal cells, while prostate cancer is an adenocarcinoma arising primarily from epithelial cells in the peripheral zone of the gland (De Nunzio et al., 2011). According to large-scale epidemiological studies, men with BPH have an elevated risk of prostate cancer and prostate cancer-related mortality (Chokkalingam et al., 2003; De Nunzio et al., 2011). However, it is still unclear whether there is a causal link between BPH and prostate cancer or if they just develop under the same pathophysiological conditions. More epidemiological studies are needed to determine the pathways connecting BPH and prostate cancer.

2.1.5 Risk factors

After age-related risks, the second largest risk factor for prostate cancer is race, and the incidence of prostate cancer varies widely between ethnic populations and countries. Asian men typically have very low incidence of prostate cancer, with age-adjusted incidence rates

ranging from 2 to 10 cases per 100,000 men (Haas et al., 2008). Higher incidence rates are generally observed in northern European countries and in the United States. African American men, however, have the highest incidence of prostate cancer in the world. In the United States, black American men have a 60% higher incidence rate than Caucasian American men (Haas et al., 2008). The reason for this is not clearly understood; African American men may have a genetic predisposition to prostate cancer, and/or the incidence is dependent on environmental factors.

Prostate cancer has a strong hereditary factor and a positive family history is the strongest risk factor after age and ethnic background. According to epidemiological studies, dominantly inherited susceptibility genes with high penetrance may cause 5 – 10% of all prostate cancer cases, and a vast majority of early onset diseases (Bratt, 2002). The lifetime risk for the development of prostate cancer increases 2-3 fold in men with one first-degree relative (father, brother) with prostate cancer (Chen YC et al., 2008). A characteristic for familial prostate cancer is that it tends to be diagnosed at a younger age than sporadic disease (Norrish AE et al., 1999).

2.1.6 Treatment

The treatment options for localized and organ-confined (localized only within the prostatic capsule) prostate cancer are active surveillance and radical prostatectomy. Active surveillance can be used because prostate cancer often grows slowly and some men might never need treatment for their prostate cancer. Organ-confined or locally spread cancer can be treated with surgery known as radical prostatectomy where the entire gland and also, if needed, some of the tissue around it are removed. Radiation therapy can be used as the first treatment for low-grade local cancer but also if the cancer has spread into nearby tissues. In advanced cancer, radiotherapy is used to reduce the size of the tumor and to relief the patient´s symptoms. The standard care for treating advanced metastatic prostate cancer is hormonal therapy. Androgen ablation therapy is used to stop the production of androgens which are important for prostate cancer to grow and develop. Unfortunately, many tumors develop resistance to hormone therapy and begin to grow and spread again after a while. Treatment options for hormone-resistant (or hormone refractory) prostate cancer are limited. (Prostate cancer: Current Care Guidelines Abstract, 2014.)

2.2 Prostate cancer genetics

Genomic instability is a fundamental feature of human cancers and a critical factor for the creation of variants within a tumor cell population. The instability drives clonal evolution and heterogeneity seen within individual tumors and among tumors of the same type, progression to malignant disease, and therapy resistance (Cahill et al., 1999). Prostate cancer is a highly heterogeneous disease in both clinically and genetically. The disease can vary from indolent, low-risk cancer to lethal castration resistant metastatic disease. The main issue in the clinics today is to segregate treatable low-risk disease from aggressive type of tumors. Overdiagnosis and overtreatment are a problem in the case of low-risk cancer leading to an inappropriate morbidity. Hence it is important to identify prognostic and predictive signatures of prostate cancer based on genomic profiles.

New screening techniques have revealed that prostate cancer is associated with multiple genomic rearrangements including somatic point mutations, small inversions and deletions, copy number alterations and gene fusions (Baca & Garraway, 2012; Tapia-Laliena et al., 2014). In addition, intrachromosomal and interchromosomal rearrangements do occur as well as extensive genome-modifying events such as chromothripsis or chromoplexy (Tapia-Laliena et al., 2014). Many potential target genes analyzed so far can be activated or deactivated by many different types of mutation. For example, variations in the androgen receptor gene expression can arise through somatic point mutations and focal amplification (Taylor et al., 2010).

2.2.1 Biomarker study of prostate cancer

Over the recent years, the amount of information about the molecular biology of cancer has increased tremendously. A great challenge is to translate this information into clinical applications. Despite the work done in the field of prostate cancer research, molecular mechanisms for the onset and progression of this disease still remain largely unknown.

Molecular biomarker can be defined as “a substance found in tissue, blood, or other body fluids that may be a sign of cancer or certain benign conditions” (National Cancer Institute, 14.2.2013). Tumor biomarkers can be specific cells, molecules, genes, gene products or hormones which can be detected from body fluids or tissues. Tumor markers are usually

present in both normal and cancerous conditions but the amount of marker to be detected is altered in malignant conditions. An optimal biomarker would be sensitive, specific and easily detected by noninvasive method e.g. from urine sample.

Molecular biomarkers can serve as useful diagnostic markers, as prognostic markers for prediction of clinical outcome and response to therapy, or as targets for new therapies. In prostate cancer research, the major goals for identifying biomarkers are to better define groups of men at high risk of developing cancer, to improve screening techniques, to distinguish indolent and aggressive disease, and to improve therapeutic strategies in patients with advanced disease.

A wide variety of putative biomarkers for prostate cancer diagnostic and prognostic have been discovered. However, due to the heterogeneous nature of the disease, there is no single biomarker described so far which would provide sufficient information of the disease independent of other information (Shariat et al., 2011). Therefore, a personalized approach could be a solution for prostate cancer dilemma. Knowledge of biomarkers could be combined with patient's individual clinical data to create a model for evaluation of disease progression and therapy opportunities.

There are many challenges in the research of novel biomarkers and to utilize them into clinical practice. First of all, the amount of data gained from numerous high-throughput studies has led to a massive increase of genomic information and identification of a myriad of candidate molecular biomarkers and therapeutic targets of prostate cancer. Each putative biomarker will require proper validation to ensure clinical utility and the validation should be performed on data not used to discover the biomarker (Sardana G et al., 2008). A standardization of analytical methodology, reference material, and quality control issues are essential to ensure the accuracy and reproducibility of the results (Bensalah et al., 2007). It has been suggested that the development of new biomarkers should follow similar principles than therapeutic drug evaluation including highly regulated phases (Shariat et al., 2011). It should be recognized that biomarker development might not be any easier than drug development and that the success rate of entering new biomarkers into clinical use is poor.

The only current and clinically approved biomarker for prostate cancer is prostate specific antigen (PSA). PSA is a serine protease produced by both normal and neoplastic epithelial

cells of the prostate and it belongs to the human kallikrein gene family. The introduction of PSA testing into clinical practice in the late 1980s and early 1990s has led to a doubling of incidence of prostate cancer and a reduction in mortality in most Western countries (Bratt & Lilja, 2015). However, at the same time, overdiagnosis and overtreatment has grown tremendously because elevated serum PSA can exist without detection of prostate cancer (Romero Otero et al., 2014). Increased serum PSA may also reflect the presence of BPH, infection or chronic inflammation. The most problematic are intermediate PSA levels which show poor correlation with grade and progression of prostate cancer (Bratt & Lilja, 2015).

2.2.2 Potential target genes in prostate cancer

Genes that are recurrently altered in prostate cancer include several important tumor suppressor genes and oncogenes such as *TP53, RB1, PTEN, MYC, PIK3CA, SPOP,* and *AR.* These genes can be affected by many different mechanisms of mutation that affect the overall expression and function of the gene product.

The androgen receptor (*AR*) regulates cellular proliferation and differentiation in the prostate epithelium in response to hormone signals. AR is a member of steroid hormone receptor transcription factor superfamily and it functions as a transcription activator of many target genes and gene networks. Human *AR* gene is located in chromosome X. The *AR* gene is frequently mutated in metastatic and castration-resistant disease (Linja & Visakorpi, 2004). However, *AR* is rarely mutated in primary tumors (Baca & Garraway, 2012). The *AR* gene expression can be altered by different mechanisms. Taylor et al. showed that *AR* gene was genetically altered by both somatic point mutations and focal amplification, and these aberrations were exclusively found in the metastatic tumor samples (Taylor et al., 2010). Furthermore, the AR collaborating factor *FOXA1* was found to be mutated in both localized and hormone-resistant prostate cancer (Grasso et al., 2012). The mutated *FOXA1* represses androgen signaling and increases tumor growth (Grasso et al., 2012).

TP53 (coding p53 protein) is frequently mutated in human cancers. p53 acts as a transcription factor in response to cellular stress such as DNA damage, and regulate different transcription pathways that ultimately lead to tumor suppression. Usually the mutation of *TP53* is loss-of-function mutation but also mutant p53 that acquire oncogenic functions have been observed in some cancers (Muller & Vousden, 2013). *TP53* mutations are more frequent in advanced

stages of prostate cancers than in early carcinoma which reflects that the mutation might be associated in the progression of prostate tumors (Isaacs & Kainu, 2001). However, even if *TP53* is one of the most commonly mutated protein-encoding genes in prostate cancer, it is still relatively rare and associated with high heterogeneity within different tumors of the same prostate gland (Isaacs & Kainu, 2001; Taylor et al., 2010).

Another commonly altered gene in prostate cancer is *PTEN* which encodes a lipid-protein phosphatase (Li et al., 1997). *PTEN*, located in 10q23, act as a part of the PI3K-PTEN-AKT signaling pathway which is aberrantly activated in prostate cancer (Baca & Garraway, 2012). Up to 70% of primary prostate cancers acquire loss of heterozygosity at the *PTEN* locus and 5-10% contains inactivating mutations (Cairns et al., 1997; Gray et al., 1998). Aberrantly activated AKT pathway due to the functional loss of *PTEN* is one the most frequent abnormalities in prostate cancer progression (de Muga et al., 2010). Somatic *PTEN* deletions and mutations have been described in advanced adenocarcinoma with the frequency of 20 to 60%, and the inactivation of the gene correlates with decreased cancer-specific survival (Baca & Garraway, 2012; de Muga et al., 2010).

MYC is a known oncogene in various cancers, and its role in prostate cancer has been also widely studied (Tapia-Laliena et al., 2014). MYC is a transcription factor with a wide range of functions in cellular growth control, differentiation and apoptosis (Hoffman & Liebermann, 2008). It is located in the chromosomal region 8q24 which is frequently amplified in prostate cancer; however, it is unclear whether *MYC* really is the candidate gene of this recurrent amplification (Fromont et al., 2013). The oncogene has been shown to be overexpressed at both mRNA and protein levels in prostate cancer (Fromont et al., 2013).

The retinoblastoma (*RB1*) tumor suppressor gene is functionally inactivated in many human cancers and it acts as a central regulator of cell cycle progression (Burkhart & Sage, 2008). RB1 maintains control of the G_1 to S-phase transition of the cell cycle primarily through interactions with the E2F family of transcription factors (Burkhart & Sage, 2008; Maddison et al., 2004). Loss of heterozygosity of the *RB* locus have been reported in 17 to 60% of prostate cancers and according to several studies the mutations of *RB1* can be early events in prostate cancer (Maddison et al., 2004). Interestingly, a recent study showing that *RB1* loss is a late event in prostate cancer suggests that *RB* deficiency may be specifically associated with the transition to castration resistant prostate cancer (Sharma et al., 2010). Also Taylor et al.

reported that loss of *RB1* is more frequent in advanced prostate cancer than in primary tumors (Taylor et al., 2010).

SPOP is a newly identified target gene in prostate cancer (Barbieri et al., 2012; Berger et al., 2011). The gene encodes a SPOP subunit which is a substrate-recognition subunit of a class of cullin E3-ubiquitin ligases. Interestingly, the tumors harboring *SPOP* mutations lack a common chromosomal rearrangement found in prostate cancer, the *TMPRSS2:ERG* gene fusion (discussed below) (Barbieri et al., 2012). The discovery of *SPOP* mutated ERG rearrangement-negative prostate cancer might define a whole new subset of prostate cancer and help to stratify the patients in the future.

2.2.3 Mutation rate and point mutations in prostate cancer

A typical feature of prostate cancer genome profile is low somatic point mutation rate. The protein-altering mutation rate in prostate cancer was found to be ~0.3 per Mb (Taylor et al., 2010), while in comparison in lung carcinoma the rate was 3.5 per Mb (Kan et al., 2010), and in malignant melanoma the frequency was found to be 30 per Mb (Berger et al., 2012). Surprisingly, there is only a moderate increase in the frequency of somatic point mutations when comparing localized and advanced prostate cancers (Grasso et al., 2012). Very few cases, however, exhibit a "hypermutated" phenotype with gross excess of point mutations which might result from alterations in DNA polymerase or DNA repair genes resulting in the accelerated rate of mutations (Kumar et al., 2011).

The genes that are recurrently altered by somatic mutations include many important tumor suppressor genes and oncogenes mentioned above, such as *TP53*, *RB1*, *PTEN*, *MYC*, and *SPOP* (Grasso et al., 2012; Taylor et al., 2010). Alteration of *AR* expression through somatic mutation is also common in prostate cancer, especially in metastatic diseases (Taylor et al., 2010). Also multiple chromatin/histone modifying genes, such as *MLL2*, have been identified to obtain recurrent point mutations (Grasso et al., 2012). In general, most prostate carcinomas are characterized by a lack of somatic driver mutations (Tapia-Laliena et al., 2014). Driver mutations are mutations that give selective advantage to cancer cell´s survival or growth in the microenvironment of the tissue in which the cancer arises. A driver mutation must have been selected at some point along cancer development but it may not be required for the maintenance of the final cancer. A major obstacle in cancer research is to distinguish genes

that carry driver mutations from those genes that obtain passenger mutations. Passenger mutations are biologically inert somatic mutations which have not been selected, have not conferred clonal growth advantage, and have therefore not contributed to cancer development. These mutations with no functional consequence will be carried in cancer genomes during cell divisions and will be present in all cells of the final cancer.

2.2.4 Copy number alterations

Copy number alterations are much more common in prostate cancer than somatic point mutations (Baca & Garraway, 2012). Multiple copy number gains and losses have been found to be associated with both localized and more advanced tumors. Comprehensive analyses have shown that these chromosomal alterations can stratify patients according to their risk for a disease recurrence and early cancer-specific mortality (Liu et al., 2013). Also, Taylor et al. showed that patients with tumors harboring no or few copy number alterations had more favorable prognosis than patients with tumors harboring excessive number of copy number alterations (Taylor et al., 2010). The challenge is to screen these altered regions and to find putative biomarkers that could be utilized in diagnosis and prognosis of the disease and that could be targeted for therapy.

The extent of copy number alterations in prostate cancer tumors increases with the disease progression, and in general, losses are more common than gains. Pre-cancerous PIN lesions contain only modest number of alterations but the frequency increases while the disease progresses from localized adenocarcinoma to metastatic disease (Zitzelsberger et al., 2001). Frequent chromosomal losses have been identified in at least chromosomes 2q, 5q, 6q, 8p, 10q, 13q, 16q, 18q, and 21q (Cheng et al., 2012). Recurrent gains have been identified in the chromosomes 3q, 7q, 8q, 9p, 17q, and Xq (Cheng et al., 2012). Few recurrent copy number alterations are concentrated in advanced tumors. For example, patients with hormone resistant prostate cancer show frequent amplification of chromosomes 7, 8q and X (Holcomb et al., 2009). Potential target genes in these regions are *AR* (X) and *MYC* (8q) (Visakorpi et al., 1995).

The most frequent copy number alterations in prostate cancer are deletions of chromosome 8p (~30-50% of cases) and gains of 8q (~20-40%) (El Gammal et al., 2010; Taylor et al., 2010). Both alterations are relatively rare in early stages of prostate cancer and the frequency of 8p

loss doesn't significantly increase from early to metastatic tumors (El Gammal et al., 2010). In contrast, the frequency of 8q gain increases steeply between early and advanced tumors indicating that the genes of this chromosome arm are relevant for the disease progression to deadly stages (El Gammal et al., 2010). The most interesting and intensively studied amplified loci on 8q region contains *MYC* gene (8q24.21) which is a frequently activated oncogene in many human cancers (Tapia-Laliena et al., 2014). Another interesting amplified gene at the 8q chromosome is the nuclear receptor coactivator gene *NCOA2* (8q13.3) which has a known role as an AR coactivator (Taylor et al., 2010).

Copy number alterations seem to have significant prognostic value in prostate cancer. For example, copy number alterations of *PTEN* and *MYC* were associated with an elevated risk for early cancer-specific mortality in a cohort of 333 men (Liu et al., 2013). Also, loss of *PTEN* together with ERG rearrangement status can predict an unfavorable prognosis of prostate cancer patients (Reid et al., 2010). These studies and many others have shown that combining different copy number alterations suitable for large-scale clinical application is a promising approach for patient risk stratification and selection of treatment choices.

2.2.4.1 A novel 9p13.3 amplicon

New small amplicon 9p13.3 (1.7 MB) was detected in prostate cancer cell lines (Kamradt et al., 2007; Taylor et al., 2010), xenografts (Leinonen, 2007, Saramaki et al., 2006; Taylor et al., 2010) and in clinical prostate tumors (Leinonen, 2007). Even 10% and 23% of prostatectomy treated patients harbor high-level and low-level 9p13.3 amplifications, respectively (Leinonen, 2007). Of hormone-refractory tumors, 14% contained high-level amplification, and 44% low-level amplification (Leinonen, 2007). The amplicon is located in the pericentromeric region of chromosome 9 and it is found by aCGH but not by cCGH due to its location near centromere (Kamradt et al., 2007; Saramaki et al., 2006).

The region 9p13.3 contains over 40 known or predicted protein coding genes and some of these genes have been studied so far to find the putative target gene or genes for this amplicon. Kamradt et al. performed a genome-wide screening for chromosomal gains and losses on nine prostate cancer cell lines using aCGH, and the 9p13.3 amplicon was detected in CWR22 and CWR22-Rv1 cell lines (Kamradt et al., 2007). To further analyze the region, they quantified the copy number of the interleukin 11 receptor alpha gene (*IL-11RA*) and the

dynactin 3 gene (*DCTN3*), and showed that the copy number gain for *IL-11RA* is higher in both cell lines and primary prostate tumors.

Saramäki et al. detected the novel amplicon in their study of genetic and expression alterations in prostate cancer (Saramaki et al., 2006). They used aCGH and found that the frequency of 9p13.3 amplification was 39% of studied prostate cancer cell lines and xenografts. When confirming the data by FISH, they found 3 genes in the amplicon region which showed significant association between increased copy number and expression. These genes were ubiquitin-conjugating enzyme *E2R2* (*UBE2R2*), member of the CDC34 family; Dynactin 3 (*DCTN3*) which encodes for subunit of dynactin, a macromolecular complex binding to both microtubules and cytoplasmic dynein; and *WDR40A,* function of which is unknown.

The 9p13.3 region was screened more precisely by Katri Leinonen in her Master´s thesis (Leinonen, 2007). The minimal region for the amplification, nearly 3.5 Mb, was determined by FISH. In order to find a putative target gene or genes for the amplicon, the mRNA expression levels and chromosomal copy number alterations for the genes in the region were screened by RT-qPCR and FISH, respectively, in 7 prostate cancer cell lines and 19 prostate cancer xenografts. The list of amplification target candidate genes was narrowed down by these methods and eight protein-coding genes passed the screening, (*C9orf25, GALT, PIGO, UBAP1, UBAP2, UBE2R2, UNC13B* and *VCP)* having the most promising correlation between gene expression levels and copy number status (unpublished results).

These genes were further studied by siRNA-mediated downregulation in cell lines with either a normal copy number status or a gain in 9p13.3 (prostate cancer cell lines PC-3 and 22Rv1; breast cancer cell lines MCF-7 and BT-474). The proliferation rate of the cells decreased significantly by downregulation of several of these genes (*GALT, PIGO, UBAP1, UBAP2, VCP*) and also invasion of PC-3 cells was altered by downregulation of *GALT* and *PIGO* (unpublished results).

2.2.5 Gene fusion

The most common genomic abnormality in prostate cancer is gene fusion *TMPRSS2:ERG*. Approximately 40 to 50% of prostate cancers harbor the fusion (Pettersson et al., 2012). The

gene fusion involves two genes located in chromosome 21; *TMPRSS2* (transmembrane protease, serine 2) and *ERG* (v-ets erythroblastosis virus E26 oncogene homolog). The oncogene *ERG* is a member of the erythroblast transformation specific (ETS) family of transcription factors which are involved in the regulation of proliferation, differentiation, apoptosis and other cellular processes (Clark & Cooper, 2009). The *TMPRSS2* gene is androgen regulated and the fusion with *ERG* leads to the formation of an androgen-responsive oncogene (Pettersson et al., 2012).

The mechanisms of the ERG fusion are only beginning to emerge but most likely involve transcription-associated DNA double-strand breaks (DBSs) (Haffner et al., 2010). It was found that androgen signaling leads to co-recruitment of AR and TOP2B (topoisomerase 2B), and TOP2B mediated DBS may be involved in the generation of *TMPRSS2:ERG* rearrangement in prostate cancer (Haffner et al., 2010). This finding is supported by another study where young men suffering from prostate cancer where found to not only have higher AR levels but also harbored ERG rearrangements more frequently than elderly patients (Weischenfeldt et al., 2013).

Despite the potential significance of *TMPRSS2:ERG* fusion, the results gained from multiple studies are controversial. A positive association between *TMPRSS2:ERG* and prostate cancer progression have been found in some studies (Attard et al., 2008; Wang et al., 2006) while others have observed null, or inverse, association (Leinonen et al., 2010; Rostad et al., 2009). It seems that the presence of *TMPRSS2:ERG* fusion itself does not correlate with progression-free or overall survival (Pettersson et al., 2012). However, when other parameters such as *PTEN* loss are combined with ERG rearrangements, the prognostic effect becomes significant (Reid et al., 2010). The presence of ERG rearrangement can be further used to subclassify prostate cancer when other cofactors are included in the analysis. For example, the mutation of *SPOP* gene occur only in *TMPRSS2:ERG* fusion-negative tumors (Barbieri et al., 2012). Furthermore, 43% of the tumors with ERG rearrangement also have *TP53* mutations and 57% have simultaneous *PTEN* loss (Barbieri et al., 2012).

2.2.6 Chromothripsis and chromoplexy

In addition to point mutations, simple translocations and focal copy number changes, complex genome rearrangements are frequently observed in cancer. In recent years, these types of

massive chromosome-damaging events have been identified also in prostate cancer (Baca et al., 2013; Berger et al., 2011). Chromothripsis is defined as an event in which structural rearrangements occur in a clustered fashion after a catastrophic chromosomal breakage (Forment et al., 2012) (Figure 4). It can involve a single chromosome or a single arm of chromosome with tens to hundreds of rearrangements. Chromothripsis has an incidence of 2-3% in a wide range of different cancers analyzed so far (Stephens et al., 2011). In contrast to chromothripsis, chromoplexy is an event involving chromosomal DNA located on multiple chromosomes (Figure 4). A massive DNA breakage event is followed by generation of chained patterns of chromosomal rearrangements and deletion bridges from up to 6 chromosomes identified so far (Baca et al., 2013). Despite the extensive DNA damage associated with both events, there is evidence suggesting that instead of accumulating sequentially over time they occur as single events (Baca et al., 2013; Stephens et al., 2011). This challenges the classical view of cancer development where mutations and genomic alterations accumulate gradually over time in pre-cancerous cells.

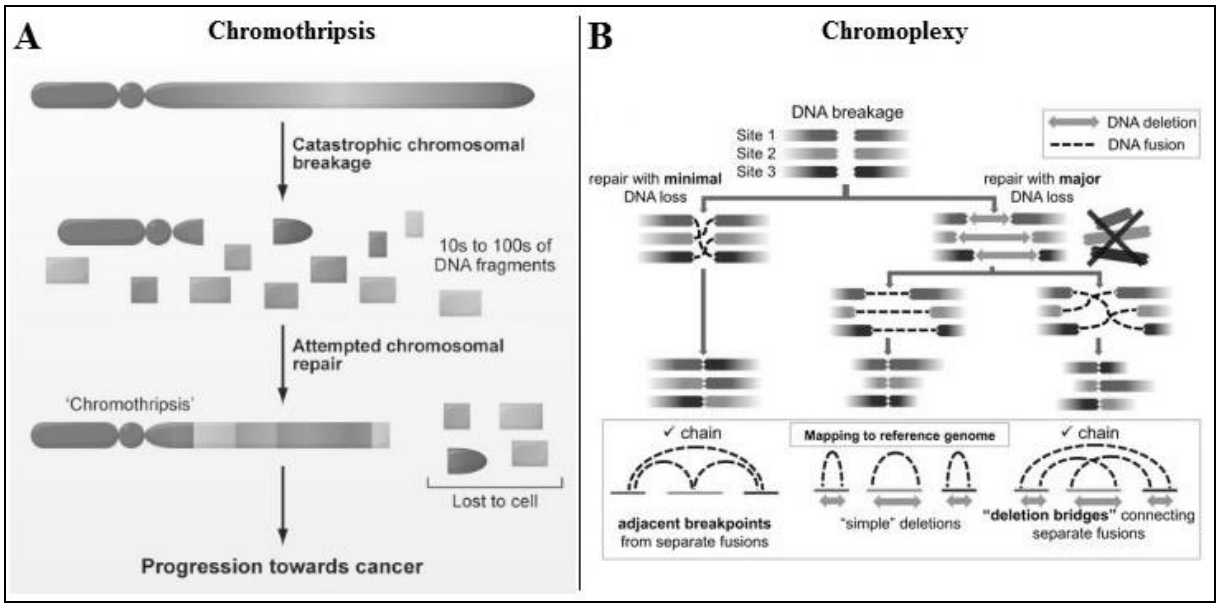

Figure 4. (A) **Chromothripsis.** A catastrophic chromosomal breakage can yield 10s to 100s of DNA fragments which are attempted to repair. Some fragments may be lost during the repair. Chromothripsis can generate several genomic lesions with potential to drive cancer in single event. (B) **Chromoplexy.** Three scenarios by which multiple DNA double-strand breaks (DSBs) may be repaired. Concerted repair with minimal loss of DNA (left) results in fusion breakpoints that map to adjacent positions in the reference genomes. Loss of DNA at sites of DSBs may result in simple deletions (middle) or "deletion bridges" (right) that span breakpoints from distinct fusions on the reference genome. Adjacent breakpoints or deletion bridges may provide evidence for chromoplexy. Pictures are modified from (A) Stephens et al., 2011 and (B) Baca et al., 2013.

As a consequence of chromothripsis and chromoplexy, the chromosomal regions are rearranged in a way that may promote carcinogenesis. This can occur if rearrangement has disrupted tumor suppressor genes and altered oncogene expression. Interestingly in prostate cancer, chromoplexy is more frequently observed in tumors containing oncogenic ERG fusion (Baca et al., 2013). ERG-overexpressing cancer cells accumulate DNA damage (Brenner et al., 2011) thereby potentially promoting chromoplexy if multiple breaks occur in spatially neighboring chromosomes.

3. AIMS OF THE RESEARCH

UNC13B could be a potential target gene for 9p13.3 amplicon and it might function as a biomarker for prostate cancer. This study is part of a broader study of 9p chromosomal region in prostate cancer. In this study the aims are to examine the function of *UNC13B* in prostate cancer and breast cancer cell lines by *UNC13B* overexpression. UNC13B protein levels will be analyzed from cancer cell lines by immunoblotting and immunofluorescence, and the functional experiments include cell growth analysis, and migration analysis. Furthermore, the expression levels of UNC13B are analyzed from clinical prostate cancer specimens by RT-qPCR and from clinical prostatectomy and hormone refractory prostate cancer tissue samples by immunohistochemistry.

4. MATERIALS AND METHODS

4.1 Cell culture

Human prostate cancer cell lines PC-3, LNCaP, DU145, 22Rv1, and human breast cancer cell line MCF-7 were obtained from American Type Culture Collection (ATCC, USA) whereas prostate cancer cell line LAPC4 was kindly provided by Dr. Charles Sawyers (Jonsson Cancer Center, UCLA, Los Angeles, USA), and prostate cancer cell lines VCaP and DuCaP were kindly provided by Dr. Jack Schalken (Radbound University Nijmegen Medical Centre, Nijmegen, The Netherlands). The cell lines were cultured under recommended conditions. The basal media used were DMEM (MCF-7), Ham's F-12 (PC-3) and RPMI 1640 (LNCaP), all purchased from Sigma-Aldrich. Basal media were supplemented with 10% fetal bovine serum (FBS) and 2 mM L-glutamine, and the cells were cultured at 37ºC and 5% CO_2.

4.2 UNC13B transfection

For functional assays, cells were transiently transfected with *UNC13B* cDNA cloned in pCMV6-XL4 expression vector (OriGene Technologies, Inc.). Transfection was performed using jetPEI® transfection reagent (Polyplus Transfection) according to manufacturer´s instruction using 500 ng of DNA per 1 cm^2 area. Briefly, the *UNC13B* cDNA was diluted and incubated in Gibco® Opti-MEM® medium (Invitrogen). The jetPEI reagent was also diluted and incubated in Opti-MEM® medium following an addition of jetPEI solution to DNA solution. The transfection solution was incubated for 12 minutes before addition to cells. pSG5 vector was used as a control.

4.3 Clinical prostate tumor specimens

Previously extracted and reversely transcribed total RNAs from clinical benign prostatic hyperplasia, prostate cancer and hormone-refractory prostate cancer tissues were used in order to define the expression levels of UNC13B by RT-qPCR. Formalin-fixed and paraffin-embedded samples of locally recurrent hormone-refractory prostate cancers and prostatectomy prostate tumors were obtained from Tampere University Hospital. Tissue microarrays (TMAs) were previously created from the cancer samples. The materials were

used in the consent of the patients and with the approvals of the ethical committee of the Tampere University Hospital and the National Authority for Medicolegal Affairs (TEO).

4.4 RNA isolation and RT-qPCR

UNC13B expression levels were analyzed with quantitative reverse transcription polymerase chain reaction (RT-qPCR) from different prostate cancer cell lines, *UNC13B* transfected cell lines, and from clinical prostate tumor specimens.

Total RNA was extracted from cells with TRI Reagent® (Molecular Research Center, Inc.) following the manufacturer´s protocol. Briefly, the cells were cultured in 6-well plate for RNA extraction. Cell densities for PC-3, LNCaP and MCF-7 cells were 200,000, 250,000 and 300,000, respectively. *UNC13B* transfection was performed one day after the seeding and cells were lysed directly in the wells by TRI reagent on the next day after transfection. Next, phase separation was performed by adding chloroform and by centrifuging at 12,000 g for 15 minutes at +4ºC. The separated aqueous phase was transferred into a fresh tube. RNA was precipitated from the aqueous phase by mixing with isopropanol and by centrifuging at 12,000 g for 8 minutes at +4ºC. The precipitated RNA pellet was washed with 75% ethanol and subsequent centrifugation at 7,500 g for 5 minutes +4ºC. Washed and air-dried RNA pellet was solubilized in nuclease-free water and stored in -70ºC.

The reverse transcription of RNA to cDNA was performed with AMV Reverse Transcriptase (Thermo Scientific). 1 µg of RNA was mixed with Fermentas Random Hexamer Primers (0.05 µg/µl; Thermo Scientific), and with sterile water. Primers were denaturated at 65ºC for 10 minutes after which the mixture was chilled on ice. A mixture was prepared from rest of the reaction components: 10 mM dNTP mix (200 µM each), 10x AMV reaction buffer (Thermo Scientific), RNase inhibitor and AMV Reverse Transcriptase (Thermo Scientific). The reverse transcription reaction was performed for 60 minutes at 42ºC following subsequent enzyme inactivation at 70ºC for 15 minutes. The reactions were stored at -70ºC.

Prior to RT-qPCR, the UNC13B primers and PCR reaction conditions were optimized by gradient PCR. Briefly, 1 µg of DNA was mixed with 10x Optimized DyNAzyme Buffer (Thermo Scientific), 10 mM dNTP mixture (200 µM each), DyNAzyme DNA polymerase (0.04 U/µl, Thermo Scientific), UNC13B primers (Proligo) and sterile H_2O. Primers used to

detect *UNC13B* were 5´-ACGCTATGCCCTGTCTCTGT-3´ and 5´-TCTGCCACTTGA GGTCATTG-3´ (Proligo). The gradient PCR reaction conditions are listed in Table 1.

Table 1. Gradient PCR conditions for UNC13B primer optimization.

Program		**Temperature (ºC)**	**Time**
Initial denaturation		94	3 min
40 cycles:	Denaturation	94	30 sec
	Annealing	gradient 50 to 60	30 sec
	Elongation	72	20 sec
Final elongation		72	5 min

Bio-Rad CFX96 Real-Time PCR equipment (Bio-Rad) was used to perform the quantitative RT-PCR. In every reaction, there were 2 µl of template, 0.125 µl of each UNC13B primer, 10 µl of Fermentas Maxima™ SYBR Green/ROX qPCR 2x Master Mix (Thermo Scientific), and 8 µl of sterile H_2O. The RT-qPCR reaction conditions used are listed in Table 2.

Table 2. The quantitative RT-PCR reaction conditions.

Program		**Temperature (ºC)**	**Time**
Denaturation		95	10 min
50 cycles:	Denaturation	95	15 sec
	Annealing	58	30 sec
	Elongation	72	30 sec
Melting:			
	Denaturation	50	30 sec
	Annealing	65	-[1]
	Elongation	To 95[1]	0.5ºC/5 sec[1]

[1]Temperature was increased from annealing temperature to 95ºC at the rate of 0.5ºC/5 sec.

The standard curve was prepared from previously extracted total RNA from LNCaP, 22RV1, and PC-3 cell lines. The RNAs were reversely transcribed and resulting cDNAs were pooled. The standard curve was prepared using 10-fold dilution series. Sterile water was used as a negative control. Expression values were normalized to housekeeping gene *TBP* (TATA binding protein). The results from RT-qPCR were confirmed by running the samples in 1% agarose gel electrophoresis. PCR results were analyzed using CFX Manager Sofware.

4.5 Protein work

4.5.1 Protein isolation

The cells were cultured in 6-well plate for protein collection. Cell densities for PC-3, LNCaP and MCF-7 cells were 200,000, 250,000 and 300,000, respectively. *UNC13B* transfection was performed as mentioned above. *UNC13B* transfection was performed one day after the seeding and cells were collected on the next day after transfection. The cells were washed three times with ice cold phosphate buffered saline (PBS) and collected with a cell scraper in 1.5 ml of cold PBS. The tubes were centrifuged 200 g 3 min at +4ºC and extra PBS was pipetted off. Cell pellets were stored in -70ºC.

The total protein was extracted using Triton lysis buffer supplemented with 25x complete protease inhibitor cocktail (Roche), 100 mM dithiothreitol (DTT, Invitrogen), and 100 mM phenylmethylsulfonyl fluoride (PMSF). Pelleted cells were suspended to lysis buffer, incubated on ice for 15 minutes and sonicated with Bioruptor™ (Diagenode Inc.). The samples were centrifuged for 10 minutes at 16 000 g at +4°C and the cleared supernatant containing the proteins was collected into a new tube. The lysates were stored in -70ºC.

The protein concentrations of the lysates were measured using colorimetric Bio-Rad *DC* Protein Assay (Bio-Rad Laboratories) according to manufacturer´s protocol. The standard curve was prepared from 10 µg/ml bovine serum albumin (BSA) using 2-fold dilution series. The absorbances of the reactions were measured at 690 nm.

4.5.2 SDS-PAGE

Proteins were separated with sodium dodecyl sulphate-polyacrylamide gel electrophoresis (SDS-PAGE). The gel consisted a 5% resolving gel and a 3% stacking gel (Table 3). Triton lysis buffer was added to the volume of the sample including 25 to 40 µg protein to reach the total volume of 30 µl. Protein samples were boiled with SDS sample buffer/DTT (3x SDS sample buffer (New England BioLabs Inc.) and 1.25M DTT) at 95˚C for 5 minutes and sample was loaded into the gel. The samples were run first at 50V for 30min to concentrate the proteins and then at 150V for 1h 30min to separate the proteins.

Table 3. The reagents of SDS-PAGE gels.

Reagent	5% resolving gel	3% stacking gel
dH_2O	5 ml	2.1 ml
1.5M Tris pH8.8	2.25 ml	-
0.5M Tris pH6.8	-	865 µl
10% SDS	180 µl	34 µl
30% Acrylamide/Bis-acrylamide	1.5 ml	340 µl
Temed (N,N,N,N'-tetramethylenediamine)	10 µl	6.6 µl
10% APS (ammonium persulfate)	40 µl	34 µl

4.5.3 Western blot

Western blot was used to evaluate the UNC13B protein amount from *UNC13B* transfected cell lines. The Immobilon-P PVDF membrane (Millipore, pore size 0.45 µm) was activated by soaking it in 100% methanol and then in transfer buffer (25 mM Tris, 190 mM glycine, 20% methanol, pH 8.3). Western blotting was performed with Trans-Blot SD Semi-Dry Transfer Cell (Bio-Rad). Blotting was performed at 50-100 Am for 1 to 1.5 hours depending on the size of the gel.

The blotted PVDF membrane was blocked with 3% BSA overnight at +4ºC. Primary antibody against UNC13B (Sigma-Aldrich) was diluted 1:600 in 0.1% Tween 20/PBS, 3% BSA and 0.1% NaN_3. The antibody was incubated at room temperature on the membrane for 1 hour following three 10 minute washes with 0.1% Tween 20/PBS. The secondary antibody, horseradish peroxidase (HRP) conjugated swine anti-rabbit (Dako Cytomation) was diluted 1:2000 in 0.1% Tween 20/PBS and 3% BSA, and incubated at room temperature for 1 hour. Washing was performed as previously mentioned. The detection of UNC13B was performed with chemiluminescence reagent (Western Blotting Luminol Reagent; Santa Cruz Biotechnology Inc) according to manufacturer's protocol. The Super RX x-ray films (Fujifilm) were exposured for 10 minutes and processed using Agfa CP1000 Film Processor (Agfa Inc.).

4.6 Fluorescence immunocytochemistry

The cells were seeded in 6-well plate containing sterile cover slides in corresponding densities: PC-3 200,000 cells, MCF-7 300,000 cells, and LNCaP 250,000 cells per well. On the next day, the cells were transfected with *UNC13B* or pSG5 as mentioned previously. 24

hours after transfection the cover slides were rinsed with 1xPBS and the cells were fixed with 4% paraformaldehyde (PFA) for 30 minutes following rinse with PBS. Permeabilization was performed with 0.5% NP-40 substitute (nonyl phenoxypolyethoxylethanol) (Sigma-Aldrich) for 5 minutes following wash with PBS, and blocking with 3% BSA/PBS for 10 minutes. Primary antibody against UNC13B (Sigma-Aldrich) was diluted 1:300 (1 µg/ml) in 3% BSA/PBS and the cover slides were incubated with the antibody in moisture chamber over night at +4°C. After the incubation the slides were washed three times 10 minutes with PBS, and incubated with secondary antibody Alexa Fluor® 594 goat anti-rabbit IgG (Invitrogen) (1:200 dilution in 3% BSA/PBS) for 1 hour at +37°C. Washes with PBS were repeated and the cover slides were mounted on microscope slides with Vectashield® Mounting Media containing DAPI (Vector Laboratories Inc.). The staining was visualized using Zeiss Axio Imager M2 fluorescence microscope.

4.7 Cell growth and migration assays

For cell growth analysis, cells were cultured in 24-well plate in corresponding densities: PC-3 20,000 cells per well, and MCF-7 50,000 cells per well. One day later the cells were transfected with *UNC13B* or pSG5 control as described above. The growth area of the cells was measured 24 hours (day 0), 72 h (day 2) or 96 h (day 3), and 144 h (day 5) after transfection by imaging the cells with Olympus IX71 inverted light microscope (Olympus) and by using Surveyor software (Objective imaging). Images were analyzed and cell surface areas were determined by using ImageJ software (version 1.42q, National Institutes of Health). For MCF-7 cells, the transfection medium was replaced with normal growth medium after 6 h incubation and also the medium was changed every day before imaging the cells because the wells contained plenty of dead cells. All experiments were performed in six replicates and repeated at least twice.

Together with imaging, the cell growth was studied using AlamarBlue® cell viability reagent (Invitrogen). The cells were cultured and transfected as described above, and treated with AlamarBlue on days 0, 2 or 3 and 5. 50 µl of the reagent was added to the cells and 100 µl samples were collected after 90 min and 180 min incubations. Absorbances of the samples were measured spectrophotometrically at 570 nm using the 2104 EnVision® Multilabel Reader (PerkinElmer). In this assay, increase or decrease in the metabolic activity of the cell culture is measured by assaying the relative absorbances of the samples.

Cell migration experiment was performed with PC-3 cells using standard wound healing assay. PC-3 cells were seeded in 24-well plate (50 000 cells per well) and 24 hours later they were transfected with *UNC13B* or pSG5 control. The cells were cultured until confluent and a scratch was made with a sterile pipet tip to the bottom of the wells. The scratches were imaged right after they were made (day 0) with Olympus IX71 inverted light microscope (Olympus) and Surveyor software (Objective imaging), and again 18 hours later (day 1). The area of the scratches was analyzed using ImageJ software (version 1.42q, National Institutes of Health). Experiment was performed in six replicates.

4.8 Immunohistochemistry

Immunostaining was performed using polyclonal rabbit antibody against UNC13B (Sigma-Aldrich). The correct conditions for UNC13B IHC staining were first optimized using two antibody dilutions (1:2500 and 1:5000) and two different buffers for antigen retrieval (natrium citrate pH 6 and Tris-EDTA pH 9). According to the optimization, antibody dilution 1:5000 and Tris-EDTA pH 9 for antigen retrieval were chosen for the experiment.

The TMA sections of 4 µm were first deparaffinized in hexane and dehydrated in absolute alcohol, followed by antigen retrieval in Tris-EDTA buffer pH 9 in autoclave at 121ºC for 30 minutes. Sections were cooled in the same buffer for 30 minutes. The antibody was diluted 1:5000 in Normal Antibody Diluent (Immunologic) and incubated +4ºC overnight. After incubation the slides were washed three times 10 minutes with 1x Tris-buffered saline (TBS). Sections were incubated with a horseradish peroxidase-conjugated secondary antibody against mouse, rabbit, and rat IgGs (Poly-HRP-GAM/R/R IgG) (PowerVision+™, ImmunoVision Technologies) for 1 hour, and bound antibody was visualized by using diaminobenzidine (DAB) chromogen (UltraVision Detection System: anti-Rabbit, HRP/DAB, Thermo Scientific) as a HRP substrate. Sections were counterstained with Harris haematoxylin (1:4 dilution, 4 min incubation). Staining without primary antibody was used as a negative control. Staining intensities were classified as negative (0), weak (1), moderate (2) and strong (3).

Previously done triple staining (AMACR/p63/keratin) was used to identify adenocarcinoma from the TMA samples. Briefly, the triple staining was performed using a cocktail of 3 antibodies, including antibodies against α-methylacyl-CoA racemase (AMACR), high molecular weight cytokeratin 34βE12, and prostate basal cell marker p63. The presence of

cancer was designated as blue cytoplasmic granular staining (AMACR) of the glandular epithelial cells in the absence of basal cells. The basal cells of benign acini had dark brown nuclear (p63) and cytoplasmic (34βE12) stainings.

4.9 Statistical analyses

Unpaired t-test or Mann-Whitney U-test was used to determine statistical difference between control and UNC13B transfected samples in functional assays. Kaplan-Meier analysis was used to test the progression free survival of prostatectomy treated patients.

5. RESULTS

5.1 The expression of *UNC13B* in cancer cell lines

The expression of endogenous *UNC13B* mRNA was determined with RT-qPCR from different prostate cancer cell lines (Figure 5). VCaP and DuCaP have the highest expression levels and 22RV1 and PC-3 have the lowest. PC-3 and LNCaP cell lines were chosen for overexpression experiments as they are commonly used models and thought to represent different stages of prostate cancer. Also, their endogenous *UNC13B* expression is rather low.

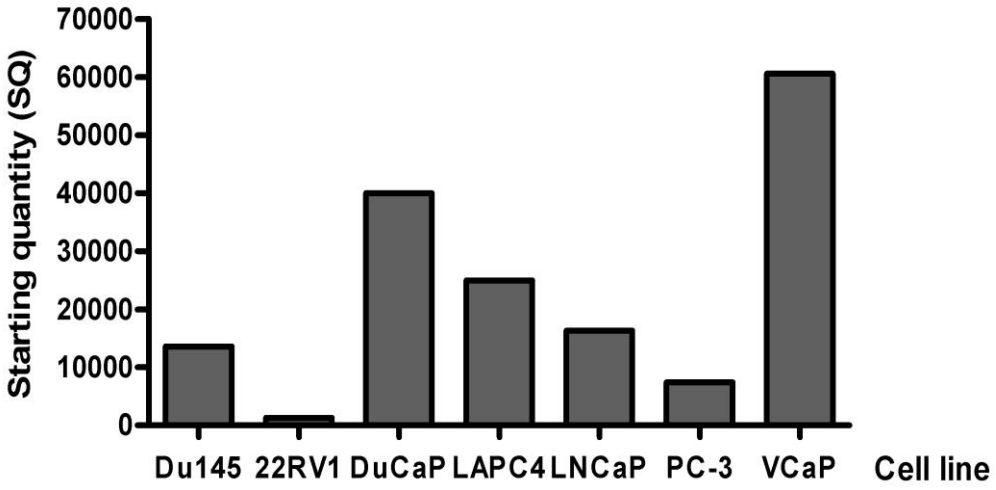

Figure 5. The expression of *UNC13B* in different prostate cancer cell lines. There is a difference between the expression levels of *UNC13B* in prostate cancer cell lines: VCaP and DuCaP have the highest levels while 22RV1 and PC-3 show lowest levels of expression.

The relative overexpression of *UNC13B* was determined with RT-qPCR from non-transfected, pSG5 transfected (control), and *UNC13B* transfected MCF-7, PC-3, and LNCaP cells (Figure 6). As expected, the expression levels of *UNC13B* in non-transfected and pSG5 transfected cells are negligible compared to the levels of overexpression in *UNC13B* transfected cells in all cell lines. Also, the levels of *UNC13B* overexpression show variability in studied cell lines. *UNC13B* expression in LNCaP is about two fold compared to MCF-7, and about four to five fold compared to PC-3.

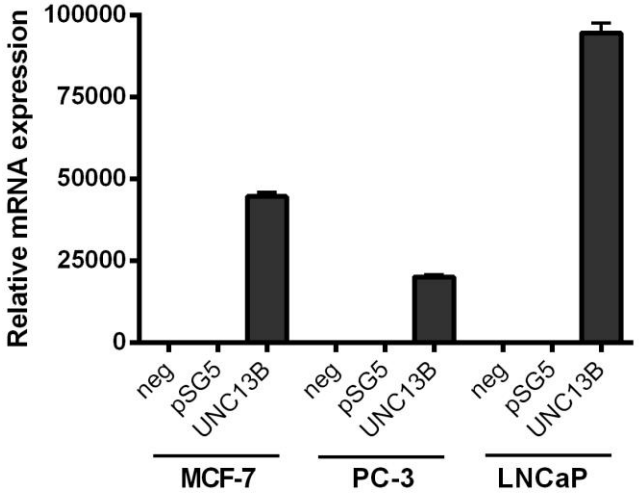

Figure 6. The relative expression levels of *UNC13B* in MCF-7, PC-3, and LNCaP cell lines. Expression levels were determined from non-transfected (neg), pSG5 transfected (control), and *UNC13B* transfected cell lines with RT-qPCR. The difference in *UNC13B* overexpression is obvious between three studied cell lines LNCaP gaining the highest level of overexpression and PC-3 the lowest. Error bars indicate standard error of the mean.

The UNC13B protein levels were determined by Western blotting from non-transfected, pSG5 transfected (control), and *UNC13B* transfected MCF-7, PC-3, and LNCaP cells (Figure 7). Endogenous UNC13B protein level is lowest in PC-3 cells. The difference at the UNC13B protein levels between control and UNC13B overexpressing samples and also between different cell lines is somewhat contrary with the results obtained from RT-qPCR. Difference in UNC13B protein levels between control and *UNC13B* transfected cells can be seen in all three cell lines. However, the difference is the greatest in MCF-7 samples where *UNC13B* overexpression yields a massive increase in UNC13B protein amount whereas according to RT-qPCR results, the overexpression status is the greatest in LNCaP cells. Overexpression status in PC-3 cells is low.

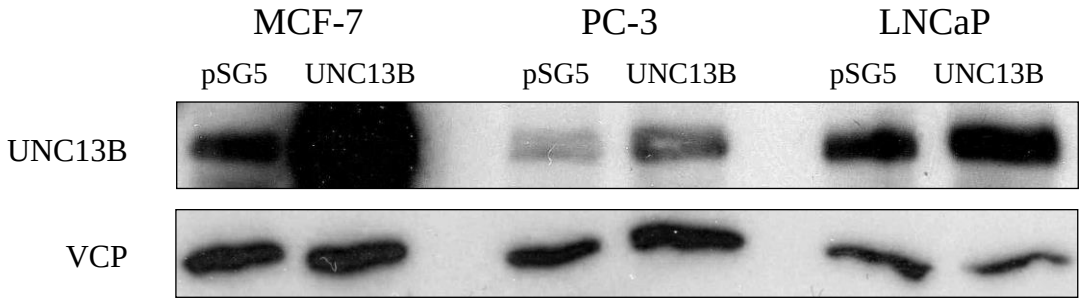

Figure 7. The quantity of UNC13B protein in control (pSG5) and *UNC13B* transfected MCF-7, PC-3, and LNCaP cell lines. There are visible differences in protein quantities between control and *UNC13B* transfected cells in all cell lines. MCF-7 gained the highest protein level under *UNC13B* overexpression. VCP was used as a loading control.

Fluorescence immunocytochemistry was applied to analyze UNC13B expression at the protein level and UNC13B localization in cancer cells. Also transfection efficiency was evaluated. According to visual observation the transfection efficiency was rather high in MCF-7 and LNCaP cells but in PC-3 cells the efficiency was significantly lower. Only few PC-3 cells were overexpressing UNC13B at the protein level. There was also variability in the UNC13B localization when overexpressed in different cell lines. In MCF-7 and LNCaP cells, UNC13B was localized mainly to the cell cytoplasm with some nuclear localization whereas in PC-3 cells the protein was localized quite evenly between the nucleus and cytoplasm. As expected, control cells (i.e. cells transfected with an empty expression vector) did not overexpress UNC13B. Representative fluorescence microscope images of transfected MCF-7, PC-3, and LNCaP cells are shown in Appendix 1.

5.2 Cell growth and migration analyses

The functional role of UNC13B was studied by overexpressing *UNC13B* in MCF-7 and PC-3 cells, and assaying the cell growth and migration ability. The effect of *UNC13B* overexpression on growth of the cells was assessed using growth curves. The representative figures shown below are plotted cell area measurements gained from the microscope pictures. Results from alamarBlue proliferation assays are not shown because they showed great variability between repeated experiments and compared to results from imaging.

5.2.1 MCF-7 cell growth

MCF-7 cells were transfected with pSG5 or *UNC13B* on day -1 and imaged on days 0, 2, and 5. Measurements gained from the microscope pictures are normalized against day 0 and plotted in Figure 8. According to analyze, overexpression of *UNC13B* caused statistically significant ($p<0.005$) decrease in the growth of the cells. However, the inhibition of cell growth could be visually seen as cell death (detached from the bottom of the plates) and not as decelerated cell growth.

5.2.2 PC-3 cell growth

PC-3 cells were transfected with *UNC13B* on day -1 and imaged on days 0, 2 and 5. Measurements gained from the microscope pictures are normalized against day 1 and plotted in Figure 9. Overexpression of *UNC13B* caused slight increase with statistical significant

difference (p<0,05) in the growth of the cells on day 2 when comparing control and *UNC13B* cells. On day 5, the difference is not statistically significant due to the high standard deviation of the mean.

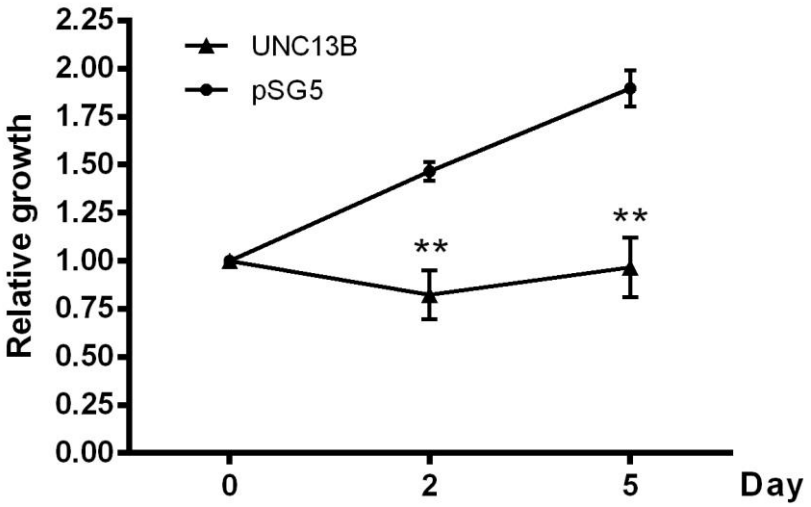

Figure 8. The effect of *UNC13B* overexpression on MCF-7 cell growth. The cells were transfected with pSG5 or *UNC13B* on day -1 and growth area was measured on days 0, 2, and 5. *UNC13B* overexpression causes decrease in the growth of the cells which results from the death of the cells. This figure is a representative example with error bars indicating +/- SD of six replicates. Measurements are normalized against day 1. **p<0.005

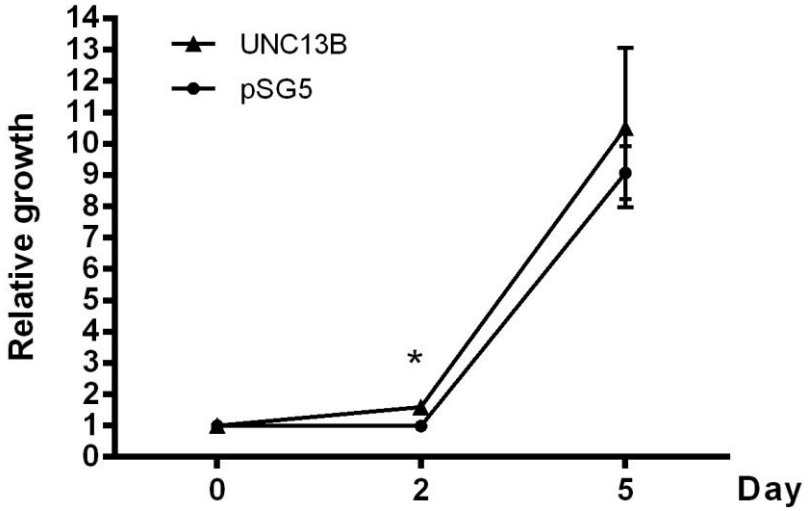

Figure 9. The effect of *UNC13B* overexpression on PC-3 cell growth. The cells were transfected with pSG5 or *UNC13B* on day -1 and imaged on days 0, 2, and 5. *UNC13B* overexpression caused statistical significant reduction of the growth on day 2 but the high standard deviation of mean on day 5 measurements disrupts the trend. This figure is a representative example with error bars indicating +/- SD of six replicates. *p<0.05

5.2.3 PC-3 cell migration

The effect of *UNC13B* overexpression to PC-3 migration ability was determined by wound healing assay. There is no difference in the migration ability of *UNC13B* transfected cells compared to control cells (Figure 10).

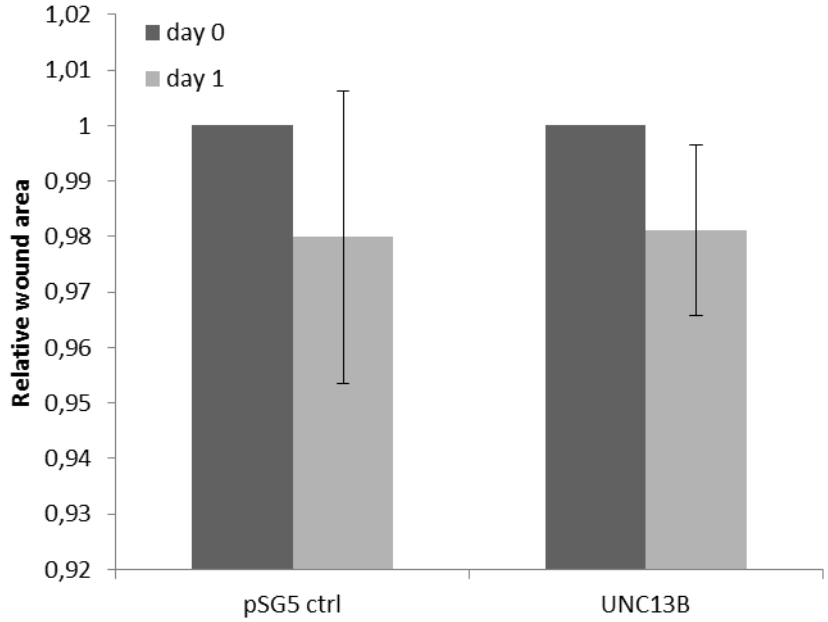

Figure 10. The effect of UNC13B overexpression on PC-3 cell migration. The cells were transfected on day -1, scratched on day 0, and imaged on days 0 and 1. Error bars indicate +/- SD of six replicates.

5.3 Results from clinical tumor sample specimens

5.3.1 RT-qPCR results

The relative expression of *UNC13B* in benign prostatic hyperplasia (BPH), untreated primary prostate cancer (PCa) and hormone refractory prostate cancer (HRPC) samples was determined by RT-qPCR (Figure 11).

There are no statistically significant differences in the expression levels between BPH and PCa samples (p=0.15) or between PCa and HRPC samples (p=0.19). However, there is a trend seen from the graph that the mean expression of *UNC13B* increases together with the disease progression. There are also more high expression cases in the HRPC population compared to BPH and PCa samples. These results indicate that *UNC13B* might have some role in the phenotype of more advanced disease.

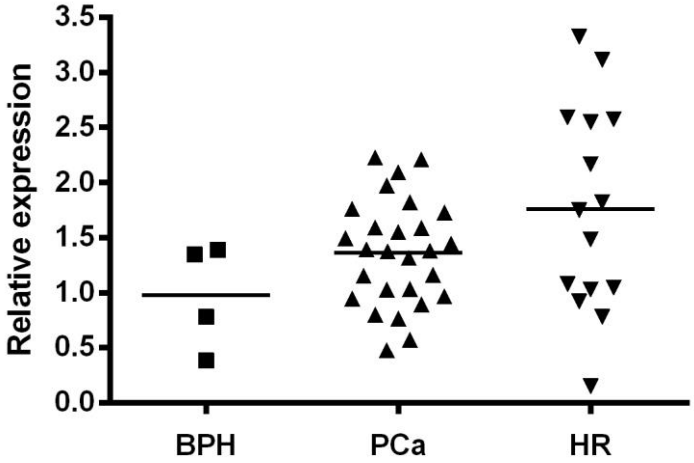

Figure 11. The relative expression of *UNC13B* in clinical prostate cancer specimens. Expression levels were determined by RT-qPCR and normalized against TBP expression levels. BPH (n=4), benign prostatic hyperplasia; PCa (n=27), untreated primary prostate cancer; HRPC (n=15), hormone-refractory prostate cancer.

5.3.2 Immunohistochemistry results

UNC13B expression was determined also at the protein level from 243 clinical prostatectomy and 115 hormone refractory prostate cancer tissue samples. IHC staining was scored from 0 to 3 according to staining intensities (Figure 12). UNC13B was expressed in glandular epithelia of prostate tissue and no stromal expression was detected. UNC13B protein was localized mainly in the cytoplasm. Both cancer tissue and PINs expressed UNC13B (verified from AMACR-p63-keratin triple stained tissue specimens). UNC13B was expressed in 236 (96%) prostatectomy samples and in 107 (96%) HRPC samples. The expression was either moderate or high in most of the tissue specimens (>80%) and the distribution of staining intensities was similar in PCa and HRPC samples (Figure 13). These results indicate that UNC13B expression is rather high in cancerous cells but it's not necessarily involved in cancer progression.

Kaplan-Meier survival analysis was made to assess the correlation between prostatectomy treated patients´ progression free survival and UNC13B expression from IHC stained samples (Figure 14). According to analysis, UNC13B expression had no statistically significant effect on progression free survival (P = 0.7466).

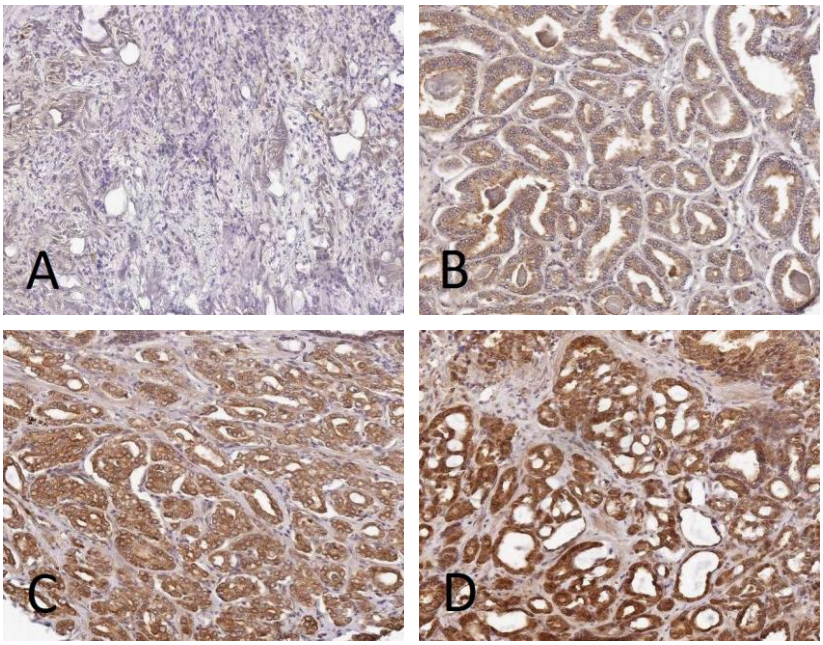

Figure 12. Different immunohistochemical staining intensities for UNC13B expression in prostate tissue specimens. A No staining (score 0) **B** Weak staining (score 1) **C** Moderate staining (score 2) **D** Strong staining (score 3). UNC13B is localized mainly in the cytoplasm of glandular epithelial cells of prostate tissue.

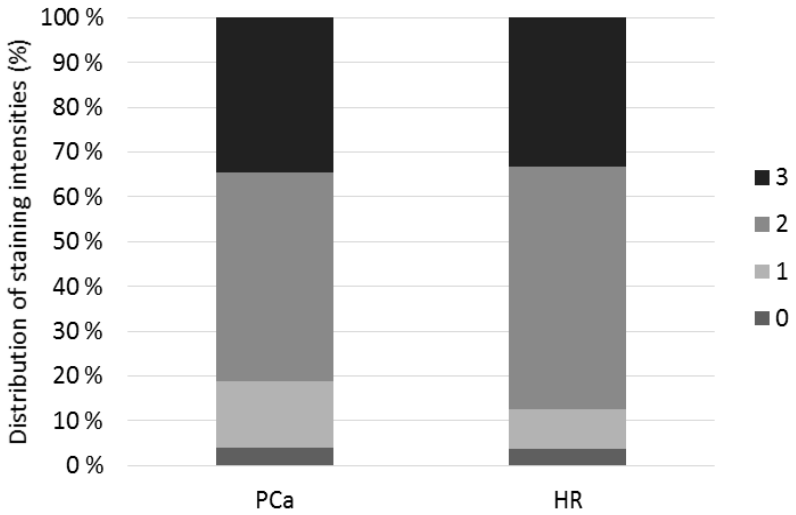

Figure 13. The distribution of UNC13B staining intensities in PCa and HRPC tissue specimens. PCa; untreated primary prostate cancer from prostatectomy specimen, HR; hormone-refractory prostate cancer specimens. Staining intensities are from no staining (0) to strong staining (3).

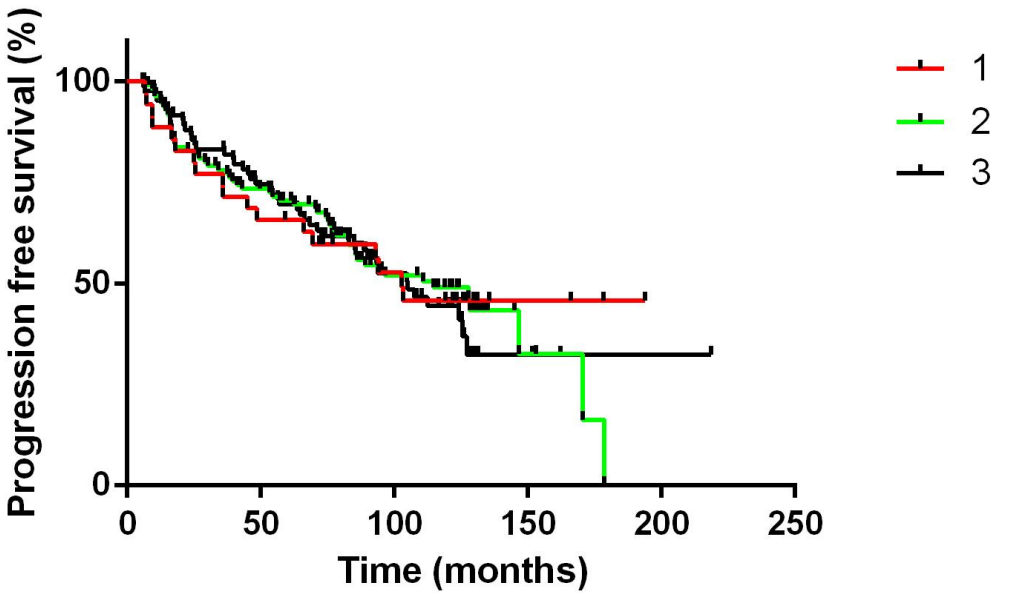

Figure 14. Progression free survival of prostatectomy-treated patients according to UNC13B. UNC13B expression had no statistically significant effect on progression free survival (P = 0.7466). Numeric values represent IHC staining intensities from low (1) to strong (3) staining.

6. DISCUSSION

The purpose of this study was to evaluate whether *UNC13B* is a potential target gene of recently found recurrent amplification in chromosomal region 9p13.3 in prostate cancer. The 9p13.3 region harbors multiple genes but none of them have known tumorigenic functions. However, mRNA expression level of some of these genes correlate with the copy number status, thus making them potential target genes of that amplification (Leinonen 2007, Taylor et al 2010). This study included *in vitro* functional experiments to see the impact of *UNC13B* overexpression to cancer cell proliferation and migration. The expression of UNC13B was also studied from clinical samples of benign prostatic hyperplasia, prostatectomy specimens and hormone refractory prostate cancer specimens at the level of mRNA and protein.

There are no previously published studies describing *UNC13B* (also known as hmunc13, munc13-2) as a putative target gene of 9p13.3 amplicon in any cancer. UNC13B belongs to a small Munc13 family that comprises of C1 domain-containing proteins within the PKC (protein kinase C) superfamily, also containing C2 and munc13 homology domains (MHD1 and MHD2) (Goldenberg and Silverman 2009). Munc13-1 through -4, have been previously studied and their roles have been identified in neurotransmitter and insulin secretion (Kabachinski et al 2014, Sheu et al 2003). In fact, Munc13 has been shown to be an essential protein for priming synaptic vesicles (Shin et al 2010). UNC13B is a cytosolic diacylglycerol (DAG) binding protein and it functions in Ca^{2+}-triggered vesicle exocytosis. Recently, hmunc13 was described as an effector of the small GTPase, rab34, which belongs to Rab family of proteins (Speight and Silverman 2005). Rab family members are involved in intracellular vesicle trafficking in addition to other important cellular processes such as signal transduction, differentiation, proliferation, nuclear assembly, and cytoskeleton formation. Recent studies have shown multiple links between Rab GTPase dysfunction and associated regulatory proteins in human diseases, including cancer (Cheng et al 2005).

6.1 The overexpression of *UNC13B* in cancer cell lines

The *UNC13B* overexpression was studied by transfecting cells with an expression plasmid carrying the *UNC13B* gene and determining both mRNA and protein levels of UNC13B in PC-3, MCF-7 and LNCaP cell lines. The overexpression was verified at the mRNA level by

RT-qPCR. The results show that studied cell lines exhibited different *UNC13B* mRNA overexpression levels. LNCaP gained the highest *UNC13B* expression and PC-3 the lowest expression. Variety in expression levels could be due to differences in transfection efficiency which may vary greatly between cell lines and depends on the transfection method.

An interesting finding was how the levels of *UNC13B* mRNA in MCF-7 and LNCaP cell lines were not correlated well with the protein levels. LNCaP showed the highest relative expression of *UNC13B* with overexpression at the mRNA level but when comparing the protein levels, MCF-7 cells exhibited extremely high amounts of protein. In addition, the difference in the quantity of protein between control transfected and *UNC13B* transfected LNCaP cells was expected be greater according to RT-qPCR results. However, the relative mRNA expression levels are not necessarily directly proportional to the expression level of the protein they code. Even relatively small changes in mRNA expression can produce large changes in the total amount of the corresponding protein present in the cell. The number of protein produced is highly dependent on translation-initiation features of the mRNA sequence and also translation efficiency of the cell.

Reasons why MCF-7 cells gained such a high UNC13B protein amount under overexpression still remains a question. This might indicate differences between different cell lines in protein degradation, stability or translation efficiency. MCF-7 cells might translate *UNC13B* mRNA more efficiently than PC-3 and LNCaP cells yielding higher amounts of protein. Also MCF-7 cells might have some defects in the protein degradation system so they can´t handle such a large amount of protein produced in a short time. For example, MCF-7 cells might lack certain activity and/or protein that is needed to degrade UNC13B. The possible disability to handle large protein amount could also explain why *UNC13B* transfected MCF-7 cells died so easily after transfection. The abnormally high protein amount might have been detrimental for the cells.

PC-3 cells gained the lowest UNC13B mRNA and protein concentrations after transfection of the cell lines analyzed. According to immunocytochemistry results only few PC-3 cells transfected with *UNC13B* actually overexpressed it. These results might arise from low transfection efficiency which is a known weakness of transient transfection method.

It might also be possible that UNC13B is under a strong post-transcriptional regulation in PC-3 cells thus leading to reduced amounts of UNC13B mRNA and protein. Possible post-transcriptional regulatory mechanisms include mRNA splicing, export, stability and translation. RNA-binding proteins are responsible for much of this regulation but other mechanisms such as non-coding RNAs are similarly involved. These regulators recognize sequence motifs in target mRNAs and tag them for recognition by macromolecular complexes involved in RNA metabolism. Cancer cells might harbor aberrant regulatory mechanisms in order to achieve growth or motility advantage over normal cells (Audic and Hartley 2004). More studies are needed to assure whether the results reflect transfection efficiency or the activity of cell´s regulatory pathways.

6.2 The effects of *UNC13B* expression on cancer cell growth and migration

In order to study the function of UNC13B in cancer cells, PC-3 and MCF-7 cells were transiently transfected with *UNC13B* cDNA. PC-3 and MCF-7 cell lines were chosen for this study because they have a normal 9p13.3 copy number status and endogenous *UNC13B* expression is low in both cell lines. Thus the overexpression analysis mimics the potential situation that the 9p13.3 amplification would increase the expression levels of *UNC13B*. The effect of *UNC13B* overexpression on cell growth was determined by cell area measurements in a designated time interval.

The effect of *UNC13B* overexpression on MCF-7 cell growth was difficult to determine due to the cells transfected with *UNC13B*, but not with pSG5, died very easily. MCF-7 cells might have suffered from the transfection mechanism of choice, although this is probably not the case because control cells grew rather normally. High protein levels were most likely the cause of MCF-7 cell death upon transfection, as discussed above. Similar effect wasn't detected neither in PC-3 nor LNCaP cell lines.

UNC13B overexpression had little effect on PC-3 cell growth. There was a small increase in the cell growth of *UNC13B* transfected PC-3 cells on growth measurement day 2 (3 days after transfection) compared to control transfected cells, however the trend was disrupted on day 5 due to the high standard deviation of mean. These results might reflect either low transfection efficiency or some features of the post-transcriptional regulation in PC-3 cells, as discussed

above. It is also possible that the function of *UNC13B* in prostate cancer cells has no direct effect on mechanisms regulating cell proliferation. More studies are needed to resolve UNC13B function in cancer cells.

Cell migration was studied with standard wound healing assay with PC-3 cells which are highly invasive cells. MCF-7 and LNCaP cells weren't included in the migration assay because of their significantly lower migration ability. PC-3 cells were transfected to overexpress *UNC13B* and the wound healing was followed for 24 hours. There was no difference in the migration ability of *UNC13B* transfected cells and control transfected cells. This might again be due to low transfection efficiency. However, the result might also indicate that *UNC13B* does not have a role in cell migration, or that the function is not so straightforward that it would be apparent in the rather simple wound healing assay.

Overexpression provides a useful tool to study gene function in cell culture. It would be interesting to see whether stable transfection of *UNC13B* to prostate cancer cells would produce different results for cell proliferation and migration assays. For stable transfection, introduced genetic material is integrated into the host genome and sustains transgene expression even after host cells replicate. In contrast, transiently transfected genes are only expressed for a limited period of time without integration into the genome. Furthermore, transiently transfected genetic material can be lost during cell division or by environmental factors. However, transient transfection is advantageous for fast and simple analysis of genes compared to laborious stable transfection which is why it was chosen for this pilot study.

6.3 UNC13B expression in clinical prostate tissue specimens

The expression of *UNC13B* was determined from clinical benign prostatic hyperplasia (BPH), prostate cancer (PCa) and hormone-refractory prostate cancer (HRPC) tissue samples which represent the transcriptome (total RNA) of a given clinical sample. The transcriptome reflects the genes that are being expressed at a given time excluding mRNAs which are degraded due to transcriptional attenuation. The relative expression of *UNC13B* was studied using RT-qPCR which is a highly sensitive method to detect even small changes in mRNA expression.

Results from this analysis indicate that increased expression of *UNC13B* may be associated with aggressive behavior of prostate cancer. However, the results are not statistically

significant. Compared to BPH and PCa, the HRPC samples showed the highest mean expression and also few cases of particularly high *UNC13B* expression which might indicate that *UNC13B* has a role in more advanced disease. There is also a wide distribution of *UNC13B* expression levels in HRPC specimens which is in parallel with the heterogeneous nature of prostate cancer. According to few previous large scale gene expression profile studies of clinical prostate cancer samples, *UNC13B* was found to be upregulated in metastatic samples compared to benign or primary prostate cancer samples (Chandran et al 2007, Varambally et al 2005, Yu et al 2004). These results also indicate that the expression of *UNC13B* might be associated with more advanced disease, and this knowledge could possibly be utilized when developing a model with other parameters to predict the aggressiveness of the disease. Unfortunately, our study material did not include metastatic prostate cancer samples. More studies are needed to assess the potential use of *UNC13B* as a prognostic biomarker.

Immunohistochemistry was applied to analyze the expression profile of UNC13B at the protein level from formalin-fixed paraffin-embedded clinical prostatectomy (n=243) and HRPC (n=115) tissue samples. UNC13B expression was evaluated according to staining intensities; no staining (0) reflecting no to negligible UNC13B expression, to strong staining (3) reflecting high UNC13B expression. UNC13B was located mainly in the cytoplasm of glandular epithelial cells and no stromal cell expression was detected. This observation seems valid since according to previous UNC13B studies, UNC13B has a role in vesicle transport. Glandular epithelial cells are specialized cells for secretion, so they obtain active vesicle transport system. Hence it seems logical that they gain higher UNC13B expression.

The UNC13B expression was compared between prostatectomy and HRPC samples in order to see if the expression is different in local versus more advanced disease. According to the results, the distribution of staining intensities was similar in prostatectomy and HRPC samples indicating that UNC13B expression is not associated with cancer progression. However, this result does not exclude it´s potential role in the early events of tumorigenesis. It would be interesting to assess the UNC13B expression in normal prostate epithelial cells using IHC in order to see whether the expression status changes between benign and malignant conditions.

Kaplan-Meier survival analysis was performed to determine whether UNC13B expression is associated with progression free survival of prostatectomy treated patients. Analysis showed no association between progression free survival and different UNC13B expression levels. This indicates that UNC13B expression does not have prognostic value when examining prostatectomy treated patients.

Immunohistochemistry is a valid technique used to detect protein localization and gene expression at the protein level in formalin-fixed tissue samples. The technique is based on specific antibody-antigen interactions and it is widely used in diagnostic and basic research to detect and localize protein biomarkers. Large cohorts can be screened relatively easy when IHC staining is combined with tissue microarray sample material. However, this technique requires proper optimization of several steps along the protocol. Antibody selection together with optimization of dilution and incubation conditions is essential, as well as choice of antigen retrieval method. Monoclonal antibodies are more specific than polyclonal antibodies, which in turn, have higher affinity and broader reactivity. Polyclonal antibodies are also prone to cross-reactivity as they are a mixed pool of immunoglobulins and recognize multiple epitopes on the same antigen. Depending on the antigen used, they can also detect different isoforms of proteins. The antibody used in this study was polyclonal raising a question whether similar results would be obtained by another UNC13B antibody.

7. CONCLUSIONS

The aim of this thesis was to study whether *UNC13B* is a potential target gene of novel recurrent 9p13.3 amplification in prostate cancer. This study included *in vitro* functional studies to test the effect of *UNC13B* overexpression to prostate cancer and breast cancer cell proliferation. In addition, the effect of overexpression to prostate cancer cell´s migration ability was analyzed.

The results suggest that *UNC13B* overexpression might slightly increase the growth of PC-3 cells. However, the repeated experiments showed variability, decreasing the reliability of the results. The overexpression of *UNC13B* didn´t have an effect on cell´s migration ability. The overexpression status in PC-3 cells proved to be low. In the case of MCF-7 cells, the effect on proliferation was difficult to assess since the overexpression of *UNC13B* yielded large amounts of protein that the cells couldn´t tolerate. In the future, the overexpression experiments should be optimized for both cell lines to increase the reliability of the results. In addition, it would be interesting to study the post-transcriptional regulatory mechanisms of UNC13B which seem to differ between cell lines based on distinct overexpression status.

The second aim of this thesis was to determine the expression of *UNC13B* in clinical prostate tumor specimens. The results indicate that higher *UNC13B* expression levels might be associated with more advanced disease and/or disease progression. This suggests that *UNC13B* expression profile could potentially be combined with other parameters to predict the aggressiveness of the disease. In the future, more studies are needed to assess the potential role of *UNC13B* in the field of prostate cancer prognostics and diagnostics.

8. REFERENCES

Attard G, Clark J, Ambroisine L, Fisher G, Kovacs G, Flohr P *et al*. (2008). Duplication of the fusion of TMPRSS2 to ERG sequences identifies fatal human prostate cancer. *Oncogene* **27:** 253-263.

Baca SC, Garraway LA. (2012). The genomic landscape of prostate cancer. *Front Endocrinol (Lausanne)* **3:** 69.

Baca SC, Prandi D, Lawrence MS, Mosquera JM, Romanel A, Drier Y *et al*. (2013). Punctuated evolution of prostate cancer genomes. *Cell* **153:** 666-677.

Barbieri CE, Baca SC, Lawrence MS, Demichelis F, Blattner M, Theurillat JP *et al*. (2012). Exome sequencing identifies recurrent SPOP, FOXA1 and MED12 mutations in prostate cancer. *Nat Genet* **44:** 685-689.

Bensalah K, Montorsi F, Shariat SF. (2007). Challenges of cancer biomarker profiling. *Eur Urol* **52:** 1601-1609.

Berger MF, Hodis E, Heffernan TP, Deribe YL, Lawrence MS, Protopopov A *et al*. (2012). Melanoma genome sequencing reveals frequent PREX2 mutations. *Nature* **485:** 502-506.

Berger MF, Lawrence MS, Demichelis F, Drier Y, Cibulskis K, Sivachenko AY *et al*. (2011). The genomic complexity of primary human prostate cancer. *Nature* **470:** 214-220.

Bostwick DG, FAU - Cheng L, Cheng L. (2012). Precursors of prostate cancer. - *Histopathology.2012 Jan;60(1):4-27.doi: 10.1111/j.1365-2559.2011.04007.x.* .

Bratt O. (2002). Hereditary prostate cancer: Clinical aspects. *J Urol* **168:** 906-913.

Bratt O, Lilja H. (2015). Serum markers in prostate cancer detection. *Curr Opin Urol* **25:** 59-64.

Brenner JC, Ateeq B, Li Y, Yocum AK, Cao Q, Asangani IA *et al*. (2011). Mechanistic rationale for inhibition of poly(ADP-ribose) polymerase in ETS gene fusion-positive prostate cancer. *Cancer Cell* **19:** 664-678.

Burkhart DL, Sage J. (2008). Cellular mechanisms of tumour suppression by the retinoblastoma gene. *Nat Rev Cancer* **8:** 671-682.

Cahill DP, Kinzler KW, Vogelstein B, Lengauer C. (1999). Genetic instability and darwinian selection in tumours. *Trends Cell Biol* **9:** M57-60.

Cairns P, Okami K, Halachmi S, Halachmi N, Esteller M, Herman JG *et al*. (1997). Frequent inactivation of PTEN/MMAC1 in primary prostate cancer. *Cancer Res* **57:** 4997-5000.

Chang SS. (2007). Treatment options for hormone-refractory prostate cancer. *Rev Urol* **9 Suppl 2:** S13-8.

Chen YC, FAU - Page JH, Page JH, FAU - Chen R, Chen R, FAU - Giovannucci E *et al*. (2008). Family history of prostate and breast cancer and the risk of prostate cancer in the PSA era. - *Prostate.2008 Oct 1;68(14):1582-91.doi: 10.1002/pros.20825.* .

Cheng I, Levin AM, Tai YC, Plummer S, Chen GK, Neslund-Dudas C *et al*. (2012). Copy number alterations in prostate tumors and disease aggressiveness. *Genes Chromosomes Cancer* **51:** 66-76.

Chokkalingam AP, Nyren O, Johansson JE, Gridley G, McLaughlin JK, Adami HO *et al*. (2003). Prostate carcinoma risk subsequent to diagnosis of benign prostatic hyperplasia: A population-based cohort study in sweden. *Cancer* **98:** 1727-1734.

Clark JP, Cooper CS. (2009). ETS gene fusions in prostate cancer. *Nat Rev Urol* **6:** 429-439.

Cohen RJ, FAU - Shannon BA, Shannon BA, FAU - Phillips M, Phillips M, FAU - Moorin RE *et al*. (2008). Central zone carcinoma of the prostate gland: A distinct tumor type with poor prognostic features. - *J Urol.2008 May;179(5):1762-7; discussion 1767.doi: 10.1016/j.juro.2008.01.017.Epub 2008 Mar 17.* .

de Muga S, Hernandez S, Agell L, Salido M, Juanpere N, Lorenzo M *et al*. (2010). Molecular alterations of EGFR and PTEN in prostate cancer: Association with high-grade and advanced-stage carcinomas. *Mod Pathol* **23:** 703-712.

De Nunzio C, Kramer G, Marberger M, Montironi R, Nelson W, Schroder F *et al*. (2011). The controversial relationship between benign prostatic hyperplasia and prostate cancer: The role of inflammation. *Eur Urol* **60:** 106-117.

El Gammal AT, Bruchmann M, Zustin J, Isbarn H, Hellwinkel OJ, Kollermann J *et al*. (2010). Chromosome 8p deletions and 8q gains are associated with tumor progression and poor prognosis in prostate cancer. *Clin Cancer Res* **16:** 56-64.

Forment JV, Kaidi A, Jackson SP. (2012). Chromothripsis and cancer: Causes and consequences of chromosome shattering. *Nat Rev Cancer* **12:** 663-670.

Fromont G, Godet J, Peyret A, Irani J, Celhay O, Rozet F *et al*. (2013). 8q24 amplification is associated with myc expression and prostate cancer progression and is an independent predictor of recurrence after radical prostatectomy. *Hum Pathol* **44:** 1617-1623.

Grasso CS, Wu YM, Robinson DR, Cao X, Dhanasekaran SM, Khan AP *et al*. (2012). The mutational landscape of lethal castration-resistant prostate cancer. *Nature* **487:** 239-243.

Gray IC, Stewart LM, Phillips SM, Hamilton JA, Gray NE, Watson GJ *et al*. (1998). Mutation and expression analysis of the putative prostate tumour-suppressor gene PTEN. *Br J Cancer* **78:** 1296-1300.

Haas GP, Delongchamps N, Brawley OW, Wang CY, de la Roza G. (2008). The worldwide epidemiology of prostate cancer: Perspectives from autopsy studies. *Can J Urol* **15:** 3866-3871.

Haffner MC, Aryee MJ, Toubaji A, Esopi DM, Albadine R, Gurel B *et al*. (2010). Androgen-induced TOP2B-mediated double-strand breaks and prostate cancer gene rearrangements. *Nat Genet* **42:** 668-675.

Harnden P, FAU - Shelley MD, Shelley MD, FAU - Coles B, Coles B, FAU - Staffurth J *et al*. (2007). Should the gleason grading system for prostate cancer be modified to account for high-grade tertiary components? A systematic review and meta-analysis. - *Lancet Oncol.2007 May;8(5):411-9.* .

Hoffman B, Liebermann DA. (2008). Apoptotic signaling by c-MYC. *Oncogene* **27:** 6462-6472.

Holcomb IN, Young JM, Coleman IM, Salari K, Grove DI, Hsu L *et al*. (2009). Comparative analyses of chromosome alterations in soft-tissue metastases within and across patients with castration-resistant prostate cancer. *Cancer Res* **69:** 7793-7802.

Hughes C, FAU - Murphy A, Murphy A, FAU - Martin C, Martin C, FAU - Sheils O *et al*. (2005). Molecular pathology of prostate cancer. - *J Clin Pathol. 2005 Jul;58(7):673-84.* .

Isaacs W, Kainu T. (2001). Oncogenes and tumor suppressor genes in prostate cancer. *Epidemiol Rev* **23:** 36-41.

Jiang J, Li J, Yunxia Z, Zhu H, Liu J, Pumill C. (2013). The role of prostatitis in prostate cancer: Meta-analysis. *PLoS One* **8:** e85179.

Kamradt J, Jung V, Wahrheit K, Tolosi L, Rahnenfuehrer J, Schilling M *et al*. (2007). Detection of novel amplicons in prostate cancer by comprehensive genomic profiling of prostate cancer cell lines using oligonucleotide-based ArrayCGH. *PLoS One* **2:** e769.

Kan Z, Jaiswal BS, Stinson J, Janakiraman V, Bhatt D, Stern HM *et al*. (2010). Diverse somatic mutation patterns and pathway alterations in human cancers. *Nature* **466:** 869-873.

Kumar A, White TA, MacKenzie AP, Clegg N, Lee C, Dumpit RF *et al*. (2011). Exome sequencing identifies a spectrum of mutation frequencies in advanced and lethal prostate cancers. *Proc Natl Acad Sci U S A* **108:** 17087-17092.
Leinonen K. The 9p13.3 amplicon in prostate cancer. 2007.

Leinonen KA, Tolonen TT, Bracken H, Stenman UH, Tammela TL, Saramaki OR *et al*. (2010). Association of SPINK1 expression and TMPRSS2:ERG fusion with prognosis in endocrine-treated prostate cancer. *Clin Cancer Res* **16:** 2845-2851.

Li J, Yen C, Liaw D, Podsypanina K, Bose S, Wang SI *et al*. (1997). PTEN, a putative protein tyrosine phosphatase gene mutated in human brain, breast, and prostate cancer. *Science* **275:** 1943-1947.

Linja MJ, Visakorpi T. (2004). Alterations of androgen receptor in prostate cancer. *J Steroid Biochem Mol Biol* **92:** 255-264.

Liu W, Xie CC, Thomas CY, Kim ST, Lindberg J, Egevad L *et al*. (2013). Genetic markers associated with early cancer-specific mortality following prostatectomy. *Cancer* **119:** 2405-2412.

Lonkar P, Dedon PC. (2011). Reactive species and DNA damage in chronic inflammation: Reconciling chemical mechanisms and biological fates. *Int J Cancer* **128:** 1999-2009.

Maddison LA, Sutherland BW, Barrios RJ, Greenberg NM. (2004). Conditional deletion of rb causes early stage prostate cancer. *Cancer Res* **64:** 6018-6025.

McNeal JE. (1981). The zonal anatomy of the prostate. - *Prostate.1981;2(1):35-49.* .

Mehik A, Hellstrom P, Lukkarinen O, Sarpola A, Jarvelin M. (2000). Epidemiology of prostatitis in finnish men: A population-based cross-sectional study. *BJU Int* **86:** 443-448.

Montironi R, FAU - Mazzucchelli R, Mazzucchelli R, FAU - Lopez-Beltran A, Lopez-Beltran A, FAU - Scarpelli M *et al*. (2011). Prostatic intraepithelial neoplasia: Its morphological and molecular diagnosis and clinical significance. - *BJU Int.2011 Nov;108(9):1394-401.doi: 10.1111/j.1464-410X.2011.010413.x.Epub 2011 Aug 26.* .

Muller PA, Vousden KH. (2013). P53 mutations in cancer. *Nat Cell Biol* **15:** 2-8.

Norrish AE, FAU - McRae CU, McRae CU, FAU - Cohen RJ, Cohen RJ, FAU - Jackson RT *et al*. (1999). A population-based study of clinical and pathological prognostic characteristics of men with familial and sporadic prostate cancer. - *BJU Int.1999 Aug;84(3):311-5.* .

Orsted DD, Bojesen SE. (2013). The link between benign prostatic hyperplasia and prostate cancer. *Nat Rev Urol* **10:** 49-54.

Pettersson A, Graff RE, Bauer SR, Pitt MJ, Lis RT, Stack EC *et al*. (2012). The TMPRSS2:ERG rearrangement, ERG expression, and prostate cancer outcomes: A cohort study and meta-analysis. *Cancer Epidemiol Biomarkers Prev* **21:** 1497-1509.

Prostate cancer (online). Current Care Guidelines. Working group set up by the Finnish Medical Society Duodecim and the Finnish Cardiac Society. Helsinki: The Finnish Medical Society Duodecim, 2014 (referred February 22, 2015). Available online at: www.kaypahoito.fi.

Raychaudhuri B, FAU - Cahill D, Cahill D. (2008). Pelvic fasciae in urology. - *Ann R Coll Surg Engl.2008 Nov;90(8):633-7.doi: 10.1308/003588408X321611.Epub 2008 Sep 22.* .

Reid AH, Attard G, Ambroisine L, Fisher G, Kovacs G, Brewer D *et al*. (2010). Molecular characterisation of ERG, ETV1 and PTEN gene loci identifies patients at low and high risk of death from prostate cancer. *Br J Cancer* **102:** 678-684.
Romero Otero J, Garcia Gomez B, Campos Juanatey F, Touijer KA. (2014). Prostate cancer biomarkers: An update. *Urol Oncol* **32:** 252-260.

Rostad K, Hellwinkel OJ, Haukaas SA, Halvorsen OJ, Oyan AM, Haese A *et al*. (2009). TMPRSS2:ERG fusion transcripts in urine from prostate cancer patients correlate with a less favorable prognosis. *APMIS* **117:** 575-582.

Russo A, La Croce G, Capogrosso P, Ventimiglia E, Colicchia M, Serino A *et al*. (2014). Latest pharmacotherapy options for benign prostatic hyperplasia. *Expert Opin Pharmacother* **15:** 2319-2328.

Saramaki OR, Porkka KP, Vessella RL, Visakorpi T. (2006). Genetic aberrations in prostate cancer by microarray analysis. *Int J Cancer* **119:** 1322-1329.

Sardana G, FAU - Dowell B, Dowell B, FAU - Diamandis EP, Diamandis EP. (2008). Emerging biomarkers for the diagnosis and prognosis of prostate cancer. - *Clin Chem.2008 Dec;54(12):1951-60.doi: 10.1373/clinchem.2008.110668.Epub 2008 Oct 16.* .

Schulz WA, FAU - Burchardt M, Burchardt M, FAU - Cronauer MV, Cronauer MV. (2003). Molecular biology of prostate cancer. - *Mol Hum Reprod.2003 Aug;9(8):437-48.* .

Shariat SF, Scherr DS, Gupta A, Bianco FJ,Jr, Karakiewicz PI, Zeltser IS *et al*. (2011). Emerging biomarkers for prostate cancer diagnosis, staging, and prognosis. *Arch Esp Urol* **64:** 681-694.

Sharma A, Yeow WS, Ertel A, Coleman I, Clegg N, Thangavel C *et al*. (2010). The retinoblastoma tumor suppressor controls androgen signaling and human prostate cancer progression. *J Clin Invest* **120:** 4478-4492.

Stephens PJ, Greenman CD, Fu B, Yang F, Bignell GR, Mudie LJ *et al*. (2011). Massive genomic rearrangement acquired in a single catastrophic event during cancer development. *Cell* **144:** 27-40.

Taichman RS, FAU - Loberg RD, Loberg RD, FAU - Mehra R, Mehra R, FAU - Pienta KJ *et al*. (2007). The evolving biology and treatment of prostate cancer. - *J Clin Invest.2007 Sep;117(9):2351-61.* .

Tapia-Laliena MA, Korzeniewski N, Hohenfellner M, Duensing S. (2014). High-risk prostate cancer: A disease of genomic instability. *Urol Oncol* .

Taylor BS, Schultz N, Hieronymus H, Gopalan A, Xiao Y, Carver BS *et al*. (2010). Integrative genomic profiling of human prostate cancer. *Cancer Cell* **18:** 11-22.

Toivanen R, Taylor RA, Pook DW, Ellem SJ, Risbridger GP. (2012). Breaking through a roadblock in prostate cancer research: An update on human model systems. *J Steroid Biochem Mol Biol* **131:** 122-131.

Verhagen PC, FAU - Tilanus MGJ, Tilanus MG, FAU - de Weger RA, de Weger RA, FAU - van Moorselaar RJA *et al*. (2002). Prognostic factors in localised prostate cancer with emphasis on the application of molecular techniques. - *Eur Urol.2002 Apr;41(4):363-71.* .
Visakorpi T, Kallioniemi AH, Syvanen AC, Hyytinen ER, Karhu R, Tammela T *et al*. (1995). Genetic changes in primary and recurrent prostate cancer by comparative genomic hybridization. *Cancer Res* **55:** 342-347.

Wang J, Cai Y, Ren C, Ittmann M. (2006). Expression of variant TMPRSS2/ERG fusion messenger RNAs is associated with aggressive prostate cancer. *Cancer Res* **66:** 8347-8351.

Wang X, Wang X, Li S, Meng Z, Liu T, Zhang X. (2014). Comparative effectiveness of oral drug therapies for lower urinary tract symptoms due to benign prostatic hyperplasia: A systematic review and network meta-analysis. *PLoS One* **9:** e107593.

Wein AJ. Campbell-Walsh Urology, 9th Edition review, Elsevier Saunders, Philadelphia, Edinburgh, 2007.

Weischenfeldt J, Simon R, Feuerbach L, Schlangen K, Weichenhan D, Minner S *et al*. (2013). Integrative genomic analyses reveal an androgen-driven somatic alteration landscape in early-onset prostate cancer. *Cancer Cell* **23:** 159-170.

Young B, Heath JW. Wheater´s functional histology, 4th Edition, Churchill Livingstone, Edinburgh, 2000.

Zitzelsberger H, Engert D, Walch A, Kulka U, Aubele M, Hofler H *et al*. (2001). Chromosomal changes during development and progression of prostate adenocarcinomas. *Br J Cancer* **84:** 202-208.

9. APPENDICES

Appendix 1. Representative fluorescence microscope images of UNC13B transfected MCF-7, PC-3, and LNCaP cells. The top row represents MCF-7 cells, the middle row PC-3 cells, and the bottom row LNCaP cells. The leftmost panel shows anti-UNC13B immunostaining in red, the middle panel nuclear DAPI staining and the rightmost panel shows merged images.